

NNLO parton distribution for the LHC

S.Alekhin (*Univ. of Hamburg & IHEP Protvino*)

- Theory
- Data selection
- PDF shape

“A critical Appraisal and Evaluation of Modern PDFs”, Accardi, et al., EPJC 76, 471 (2016)

sa, Blümlein, Moch, Plačakytė PRD 96, 014011 (2017)

sa, Kulagin, Petti PRD 96, 054005 (2017)

sa, Blümlein, Moch PLB 777, 134 (2018)

sa, Blümlein, Moch hep-ph/1803.07537

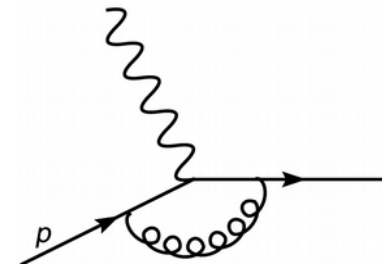
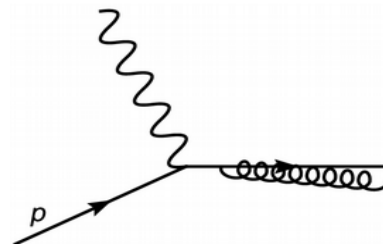
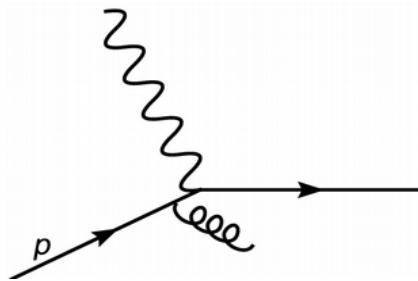
Reminder: factorization formalism

QPM: electro-production inclusive structure function

$$F_2(x, Q^2) = \sum_q e_q^2 p_q(x)$$

$p_q(x)$ – parton probability distributions (PDFs)

QCD radiative corrections:

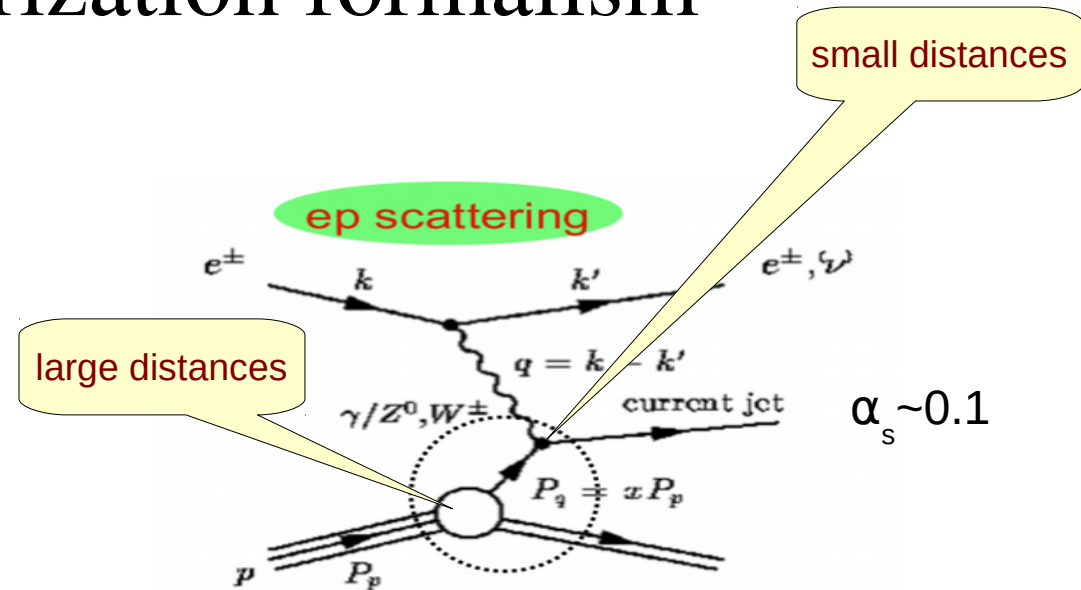


Mass singularity $\ln(Q/m_q)$ appears for the (almost) massless partons, however, it can be absorbed into PDFs \Rightarrow *PDF evolution, better theoretical accuracy, scheme dependence of PDFs and coefficient functions (partonic c.s.)*

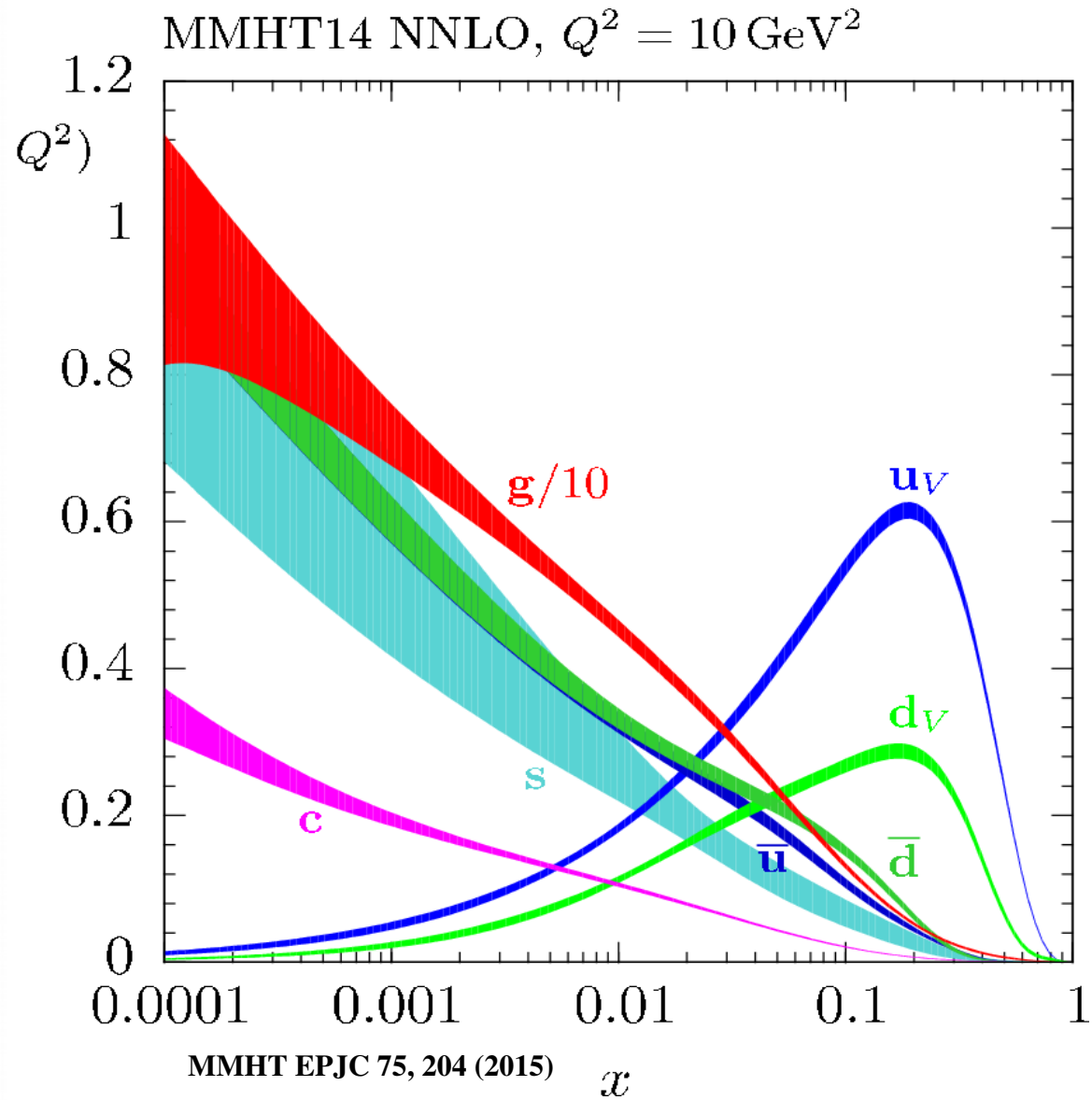
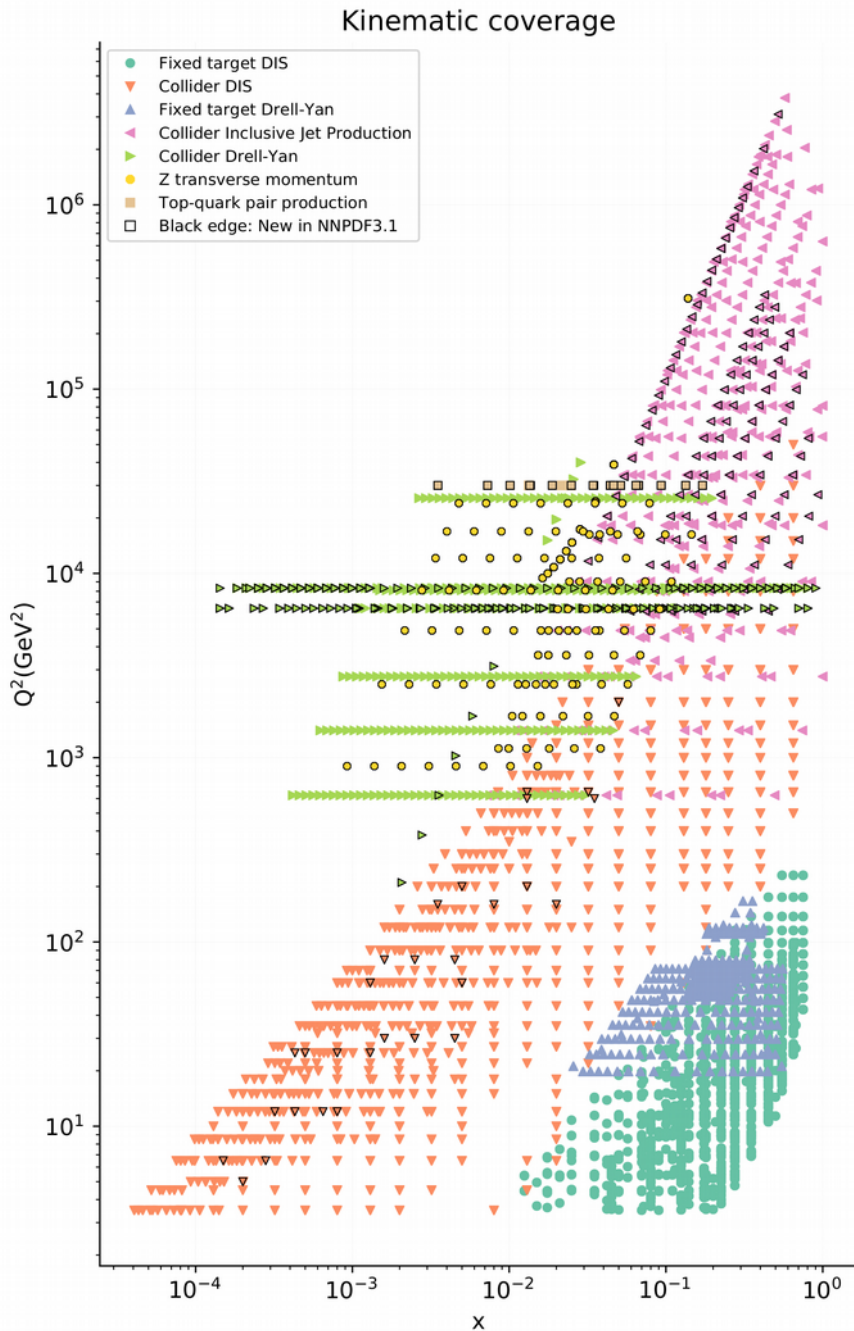
State-of-art:

NNLO Moch, Vermaseren Vogt NPB 688, 101 (2004); NPB 691, 129 (2004)

N3LO Moch et al. JHEP 1710, 041 (2017); Velizhanin hep-ph/1411.1331; Baikov, Chetyrkin NPPS 160, 76 (2006)



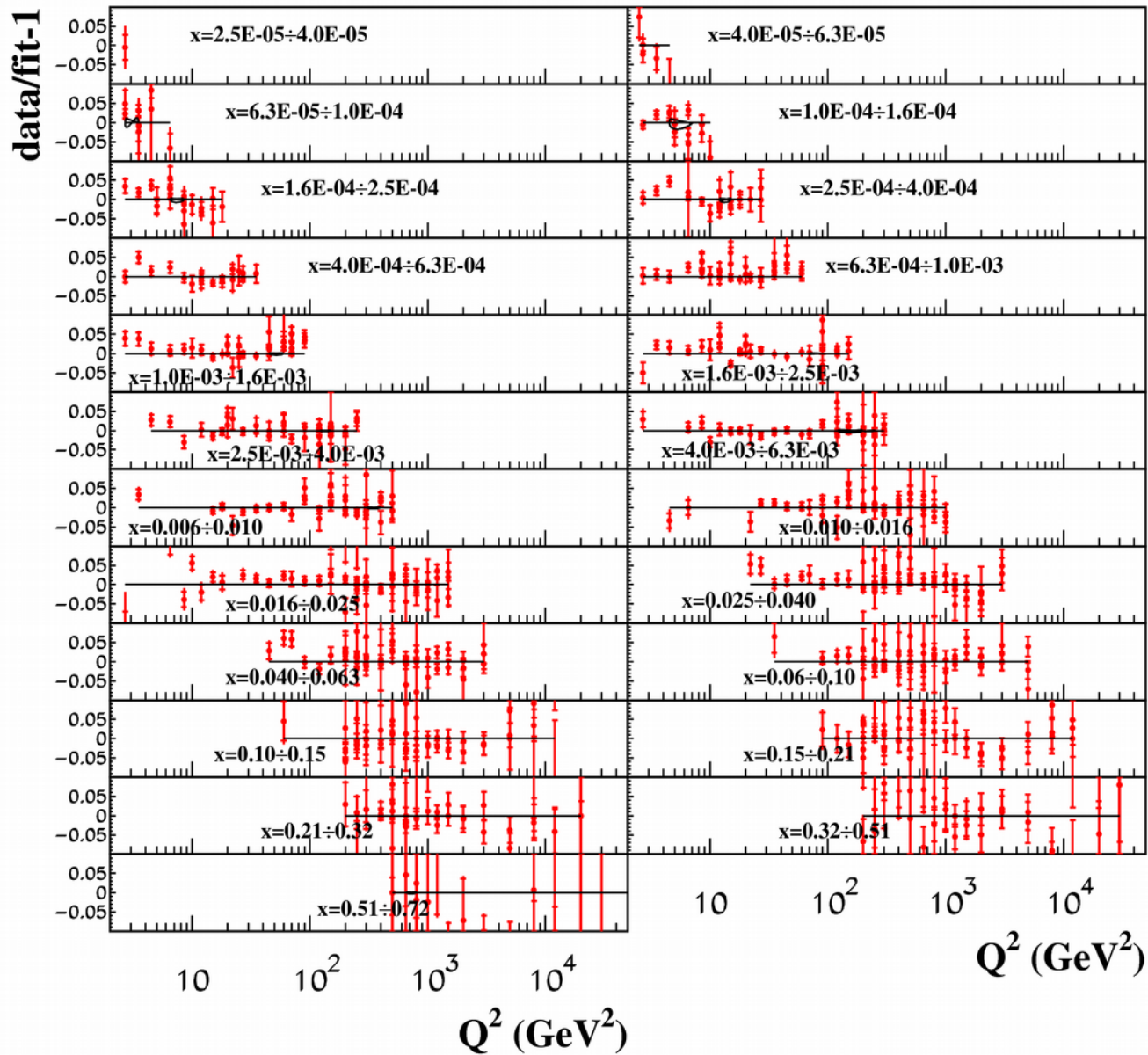
Global PDF fits



Comined Run I+II HERA data

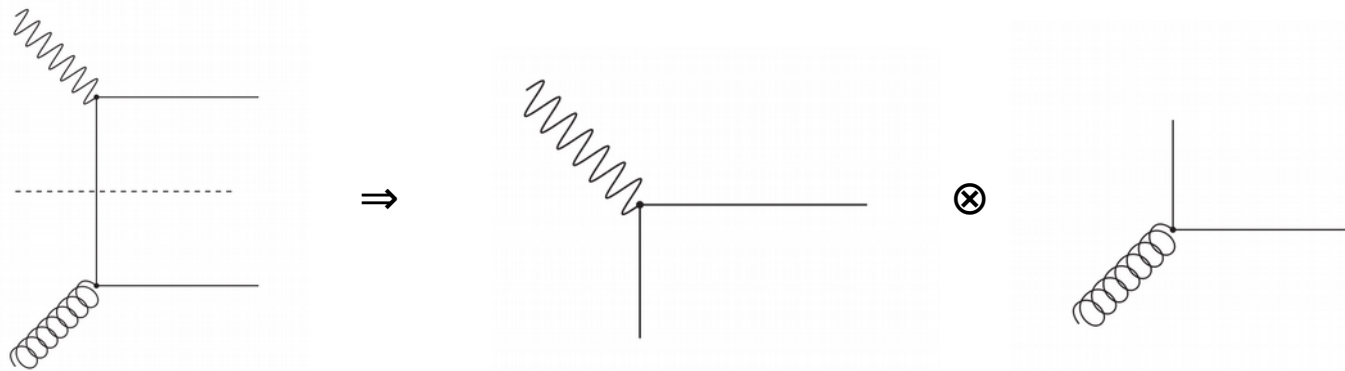
HERA I+II (NC, e^+p)

H1 and ZEUS EPJC 75, 580 (2015)



Contribution of c-quarks up to 30% at small $x \Rightarrow$ accurate treatment is required

FFN and VFN schemes



Collins, Tung NPB 278, 934 (1986)

$$H_{g,2}^{\text{asympt}} = a_s(N_f) A_{hg}^{(1)} \quad \text{Asymptotic 3-flavor coefficient function}$$

LO: $A_{ij}^{(1)}\left(z, \frac{m_h^2}{\mu^2}\right) = a_{ij}^{(1,1)}(z) \ln\left(\frac{\mu^2}{m_h^2}\right)$ Massive operator matrix elements (OMEs)

$$h^{(1)}(x, \mu^2) = a_s(N_f + 1, \mu^2) \left[A_{hg}^{(1)}\left(\frac{m_h^2}{\mu^2}\right) \otimes G^{(2)}(N_f, \mu^2) \right](x) \quad \text{Matching condition for the heavy-quark PDFs}$$

$$F_{g,2}^{\text{asympt}} = e_h^2 x h^{(1)}(x, \mu^2)$$

NLO: ...

Buza, Matiounine, Smith, van Neerven EPJC 1, 301 (1998)

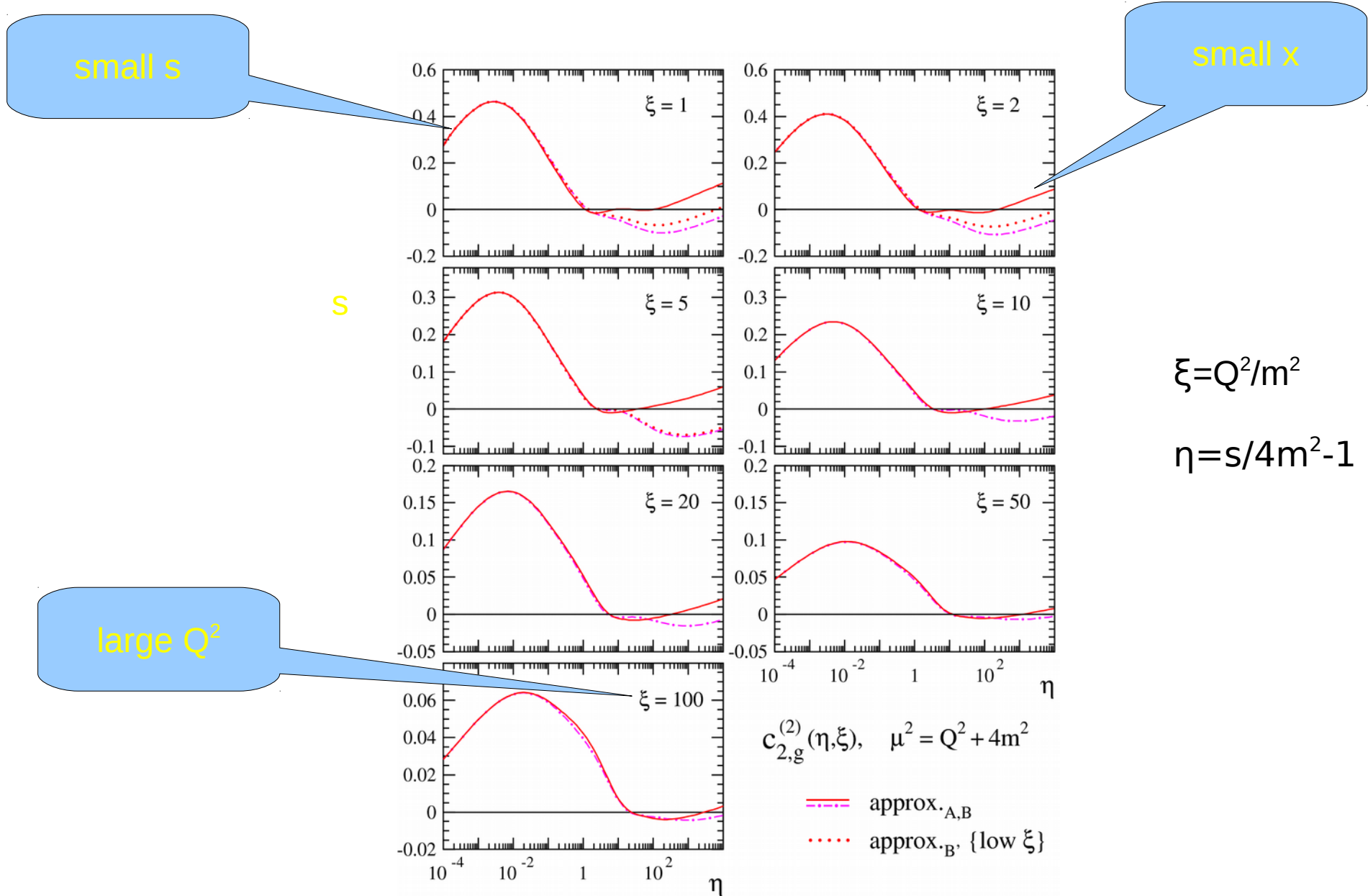
$$A_{ij}^{(2)}\left(z, \frac{m_h^2}{\mu^2}\right) = a_{ij}^{(2,2)}(z) \ln^2\left(\frac{\mu^2}{m_h^2}\right) + a_{ij}^{(2,1)}(z) \ln\left(\frac{\mu^2}{m_h^2}\right) + a_{ij}^{(2,0)}(z)$$

NNLO: log-terms; constant terms up to the gluonic one

Blümlein, et al., work in progress

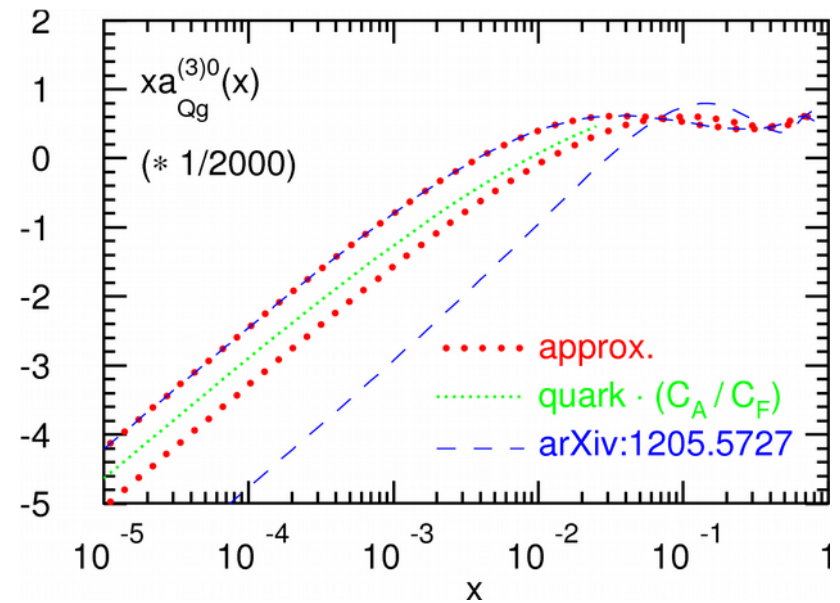
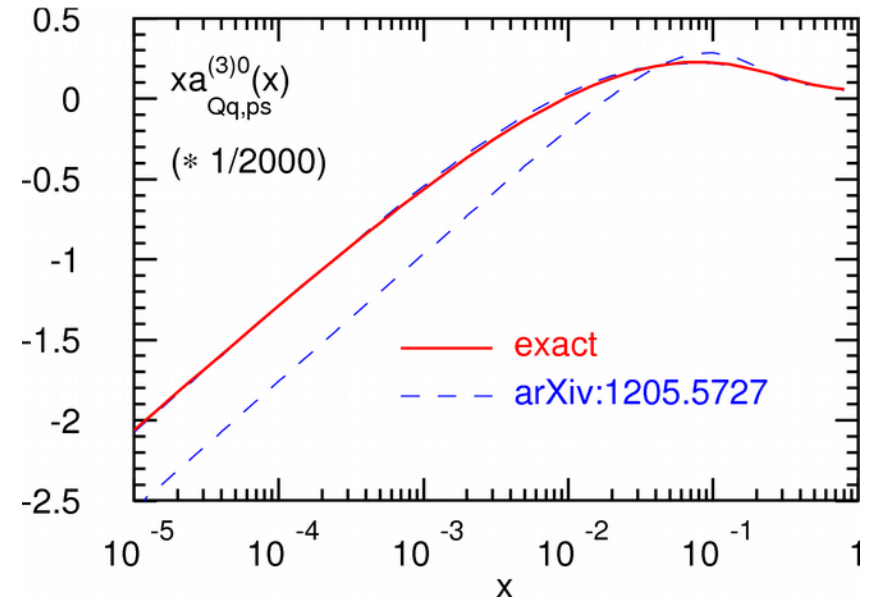
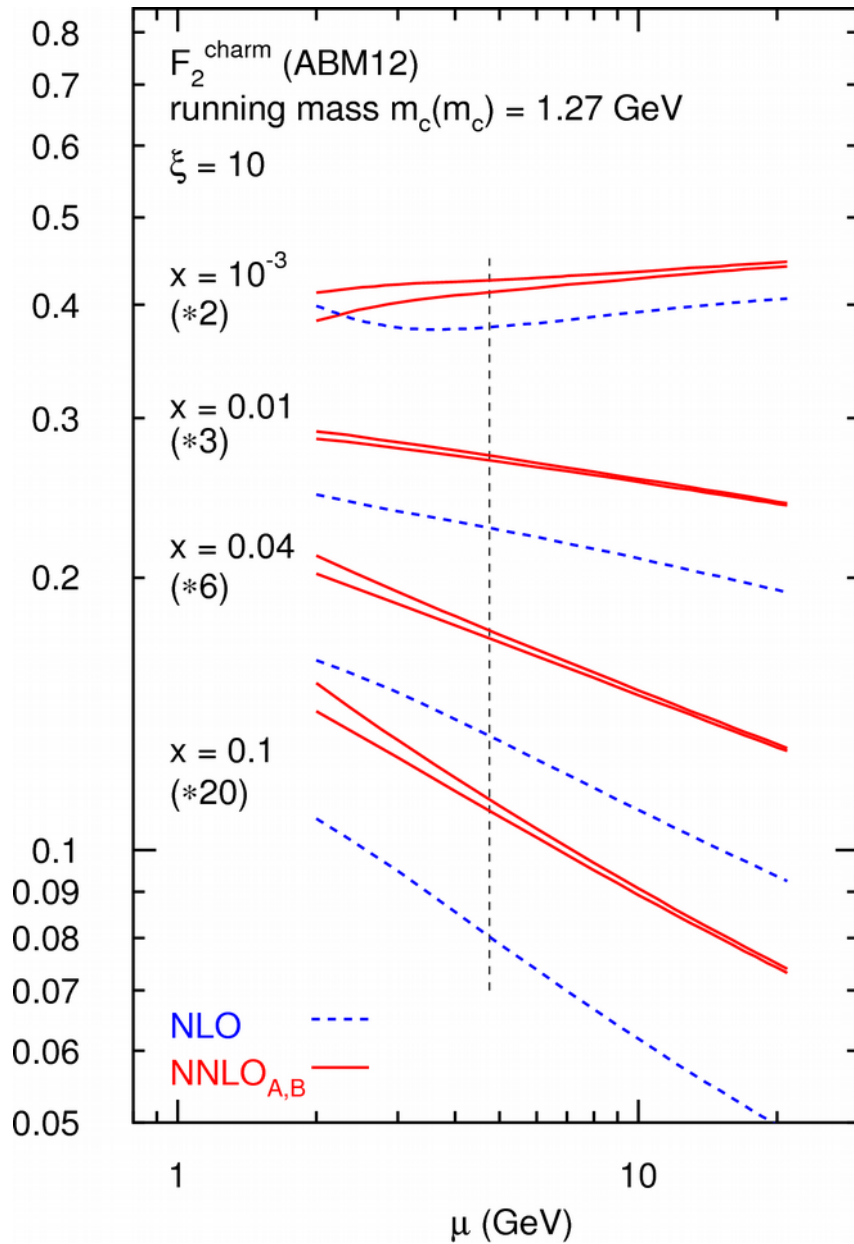
- The VFN scheme works well at $\mu \gg m_h$ (W,Z,t-quark production,....)
- Problematic for DIS \Rightarrow additional modeling of power-like terms required (ACOT, BMSN, FONLL, RT....)

Modeling NNLO FFN massive coefficients



Combination of the threshold corrections (small s), high-energy limit (small x), and the NNLO massive OMEs (large Q^2)

Recent progress in massive DIS coefficients

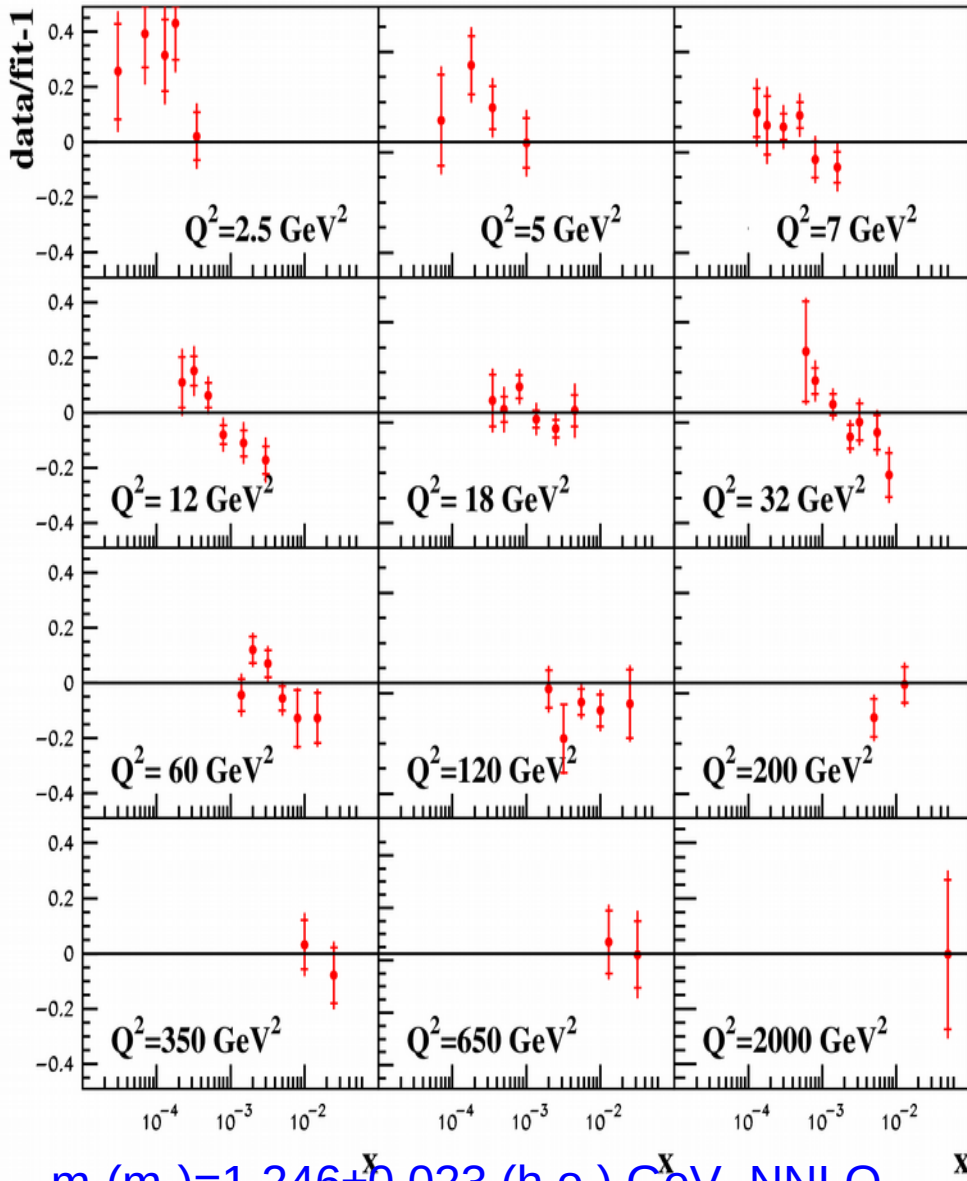


Update with the pure singlet massive OMEs → improved theoretical uncertainties

HERA charm data and $m_c(m_c)$

H1/ZEUS ZPC 73, 2311 (2013)

HERA I+II (ep \rightarrow e charm X)



$m_c(m_c) = 1.246 \pm 0.023$ (h.o.) GeV NNLO

Kiyo, Mishima, Sumino PLB 752, 122 (2016)

$m_c(m_c) = 1.279 \pm 0.008$ GeV

Kühn, this conference

$X^2/NDP = 66/52$

$m_c(m_c) = 1.252 \pm 0.018$ (exp.) - 0.01 (th.) GeV

ABMP16

$m_c(\text{pole}) \sim 1.9$ GeV (NNLO)

Marquard et al. PRL 114, 142002 (2015)

- RT optimal
 $X^2/NDP = 82/52$
 $m_c(\text{pole}) = 1.25$ GeV

NNLO

MMHT14 EPJC 75, 204 (2015)

- S-ACOT- χ
 $X^2/NDP = 59/47$
 $m_c(\text{pole}) = 1.3$ GeV

NNLO

CT14 PRD 93, 033006 (2016)

- FONLL
 $X^2/NDP = 60/47$
 $m_c(\text{pole}) = 1.275$ GeV

NNLO

NNPDF3.0 JHEP 504, 040 (2015)

- FONLL
 $X^2/NDP = 54/37$
 $m_c(\text{pole}) = 1.51$ GeV, intrinsic (fitted) charm

NNLO

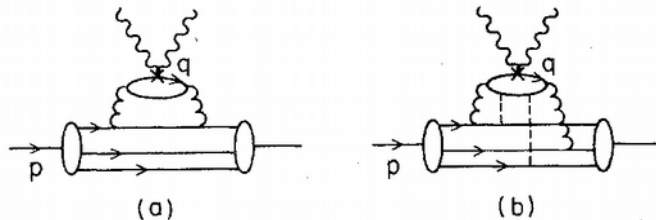
NNPDF3.1 hep-ph/1706.00428

FFNS works better, particularly at small Q

H1, ZEUS hep-ph/1804.01019

Intrinsic charm: pitfalls

- **No mass singularities** for massive partons \Rightarrow collinear QCD evolution does not work
- The mass singularities $\sim \ln(\mu/m_h)$ appear at $\mu \gg m_h$ and the evolution restores. New charm(bottom) quark distribution may be introduced, however, extrapolation to smaller scales is still problematic
- Intrinsic charm is often introduced within the VFN framework \Rightarrow interplay with the “standard” VFN modeling of power-like terms
- Original formulation of the intrinsic charm implies its power-like behavior;



Brodsky, Peterson, Sakai PRD 23, 2745 (1981)

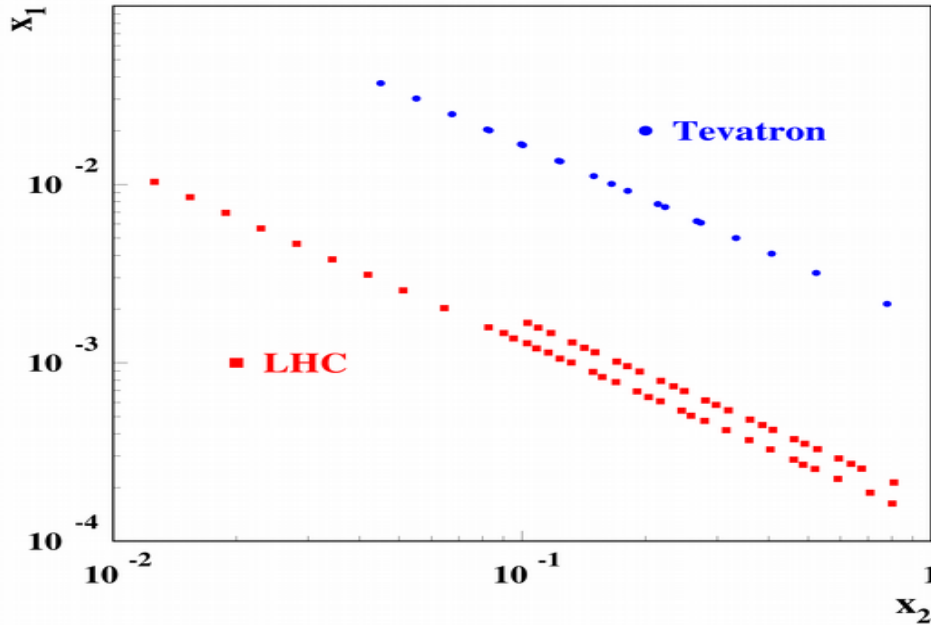
FIG. 7. (a) Example with contribution to the deep-inelastic structure functions from an extrinsic quark q ; (b) from an intrinsic quark q .

strong constraint on such terms was obtained from analysis of the EMC data on charm production

Jimenez-Delgado, Hobbs, Londergan, Melnitchouk PRL 114, 082002 (2015)

DY data in the ABMP16 fit

sa, Blümlein, Moch, Plačakytė PRD 96, 014011 (2017)



In the forward region $x_2 \gg x_1$

$$\sigma(W^+) \sim u(x_2) \text{dbar}(x_1)$$

$$\sigma(W^-) \sim d(x_2) \text{ubar}(x_1)$$

$$\sigma(Z) \sim Q_u^2 u(x_2) \text{ubar}(x_1) + Q_d^2 d(x_2) \text{dbar}(x_1)$$

$$\sigma(\text{DIS}) \sim q_u^2 u(x_2) + q_d^2 d(x_2)$$

Forward W&Z production probes small/large x and is complementary to the DIS \Rightarrow good quark disentangling

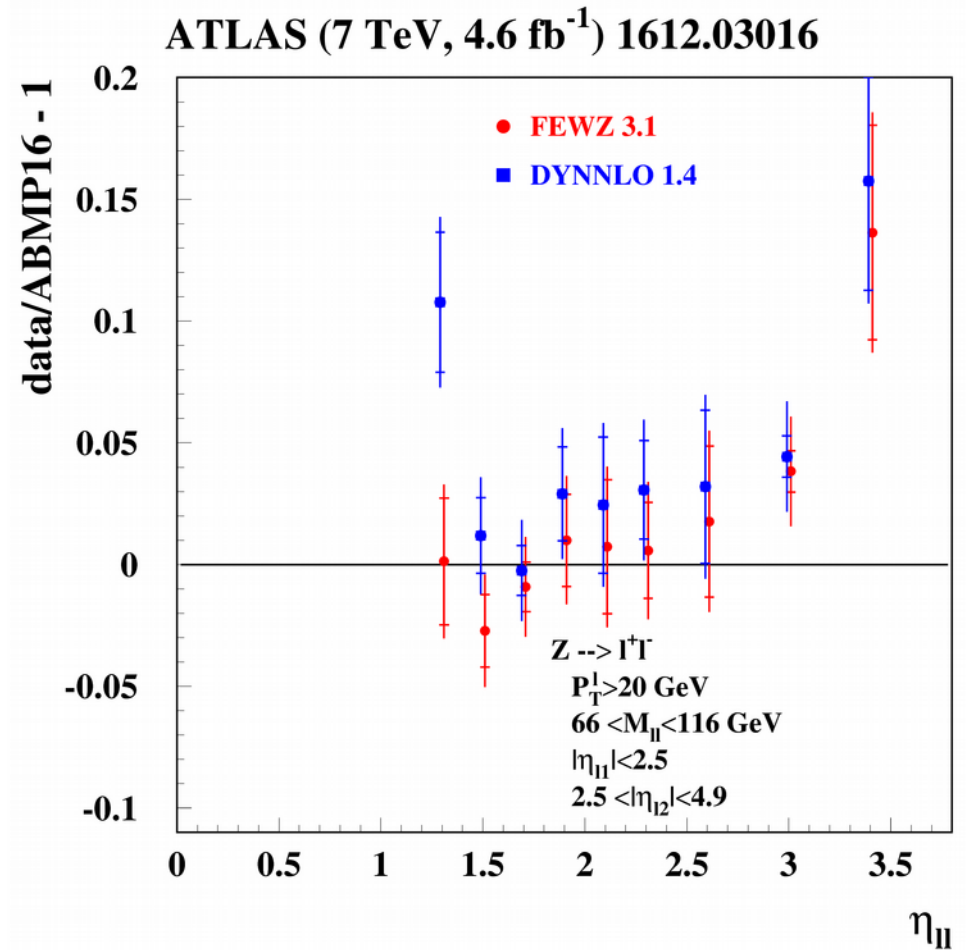
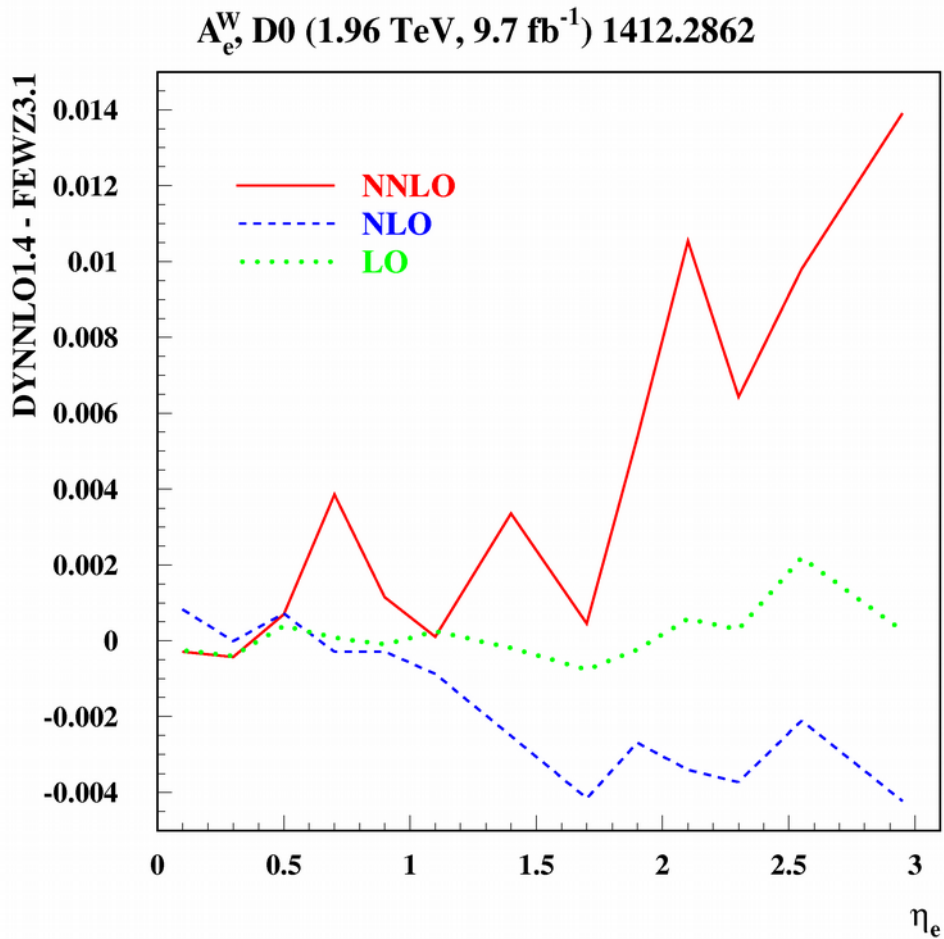
Experiment	ATLAS		CMS		DØ		LHCb			
\sqrt{s} (TeV)	7	13	7	8	1.96		7	8		
Final states	$W^+ \rightarrow l^+ \nu$ $W^- \rightarrow l^- \nu$ $Z \rightarrow l^+ l^-$	$W^+ \rightarrow l^+ \nu$ $W^- \rightarrow l^- \nu$ $Z \rightarrow l^+ l^-$	$W^+ \rightarrow \mu^+ \nu$ $W^- \rightarrow \mu^- \nu$ (asym)	$W^+ \rightarrow \mu^+ \nu$ $W^- \rightarrow \mu^- \nu$	$W^+ \rightarrow \mu^+ \nu$ $W^- \rightarrow \mu^- \nu$ (asym)	$W^+ \rightarrow e^+ \nu$ $W^- \rightarrow e^- \nu$ (asym)	$W^+ \rightarrow \mu^+ \nu$ $W^- \rightarrow \mu^- \nu$ $Z \rightarrow \mu^+ \mu^-$	$Z \rightarrow e^+ e^-$	$W^+ \rightarrow \mu^+ \nu$ $W^- \rightarrow \mu^- \nu$ $Z \rightarrow \mu^+ \mu^-$	
Cut on the lepton P_T	$P_T^l > 20$ GeV	$P_T^e > 25$ GeV	$P_T^\mu > 25$ GeV	$P_T^\mu > 25$ GeV	$P_T^\mu > 25$ GeV	$P_T^e > 25$ GeV	$P_T^\mu > 20$ GeV	$P_T^e > 20$ GeV	$P_T^\mu > 20$ GeV	
Luminosity (1/fb)	0.035	0.081	4.7	18.8	7.3	9.7	1	2	2.9	
NDP	30	6	11	22	10	13	31(33) ^a	17	32(34)	
	ABMP16	31.0	9.2	22.4	16.5	17.6	19.0	45.1(54.4)	21.7	40.0(59.2)
	CJ15	-	-	-	-	20	29	-	-	-
	CT14	42	-	- ^b	-	-	34.7	-	-	-
	HERAFitter	-	-	-	-	13	19	-	-	-
	MMHT16	39 ^c	-	-	21	21 ^c	26	(43)	29	(59)
	NNPDF3.1	29	-	19	-	16	35	(59)	19	(47)

^a The values of NDP and χ^2 correspond to the unfiltered samples.

^b For the statistically less significant data with the cut of $P_T^\mu > 35$ GeV the value of $\chi^2 = 12.1$ was obtained.

^c The value obtained in MMHT14 fit.

NNLO tools benchmarking

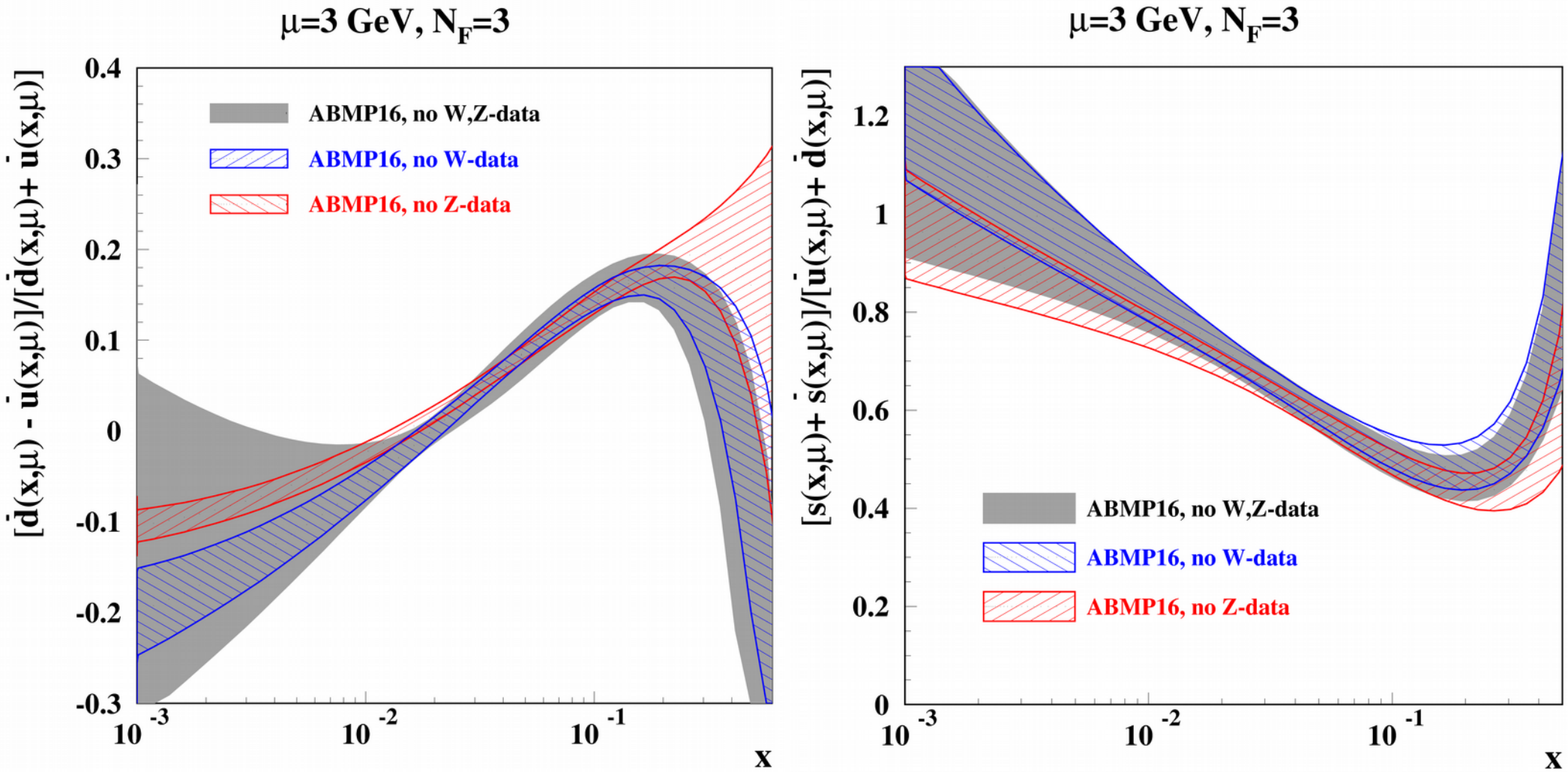


Yannick Ulrich, Bachelor thesis, Univ. of Hamburg 2015

DYNNLO-FEWZ difference not fully understood; further benchmarking is needed

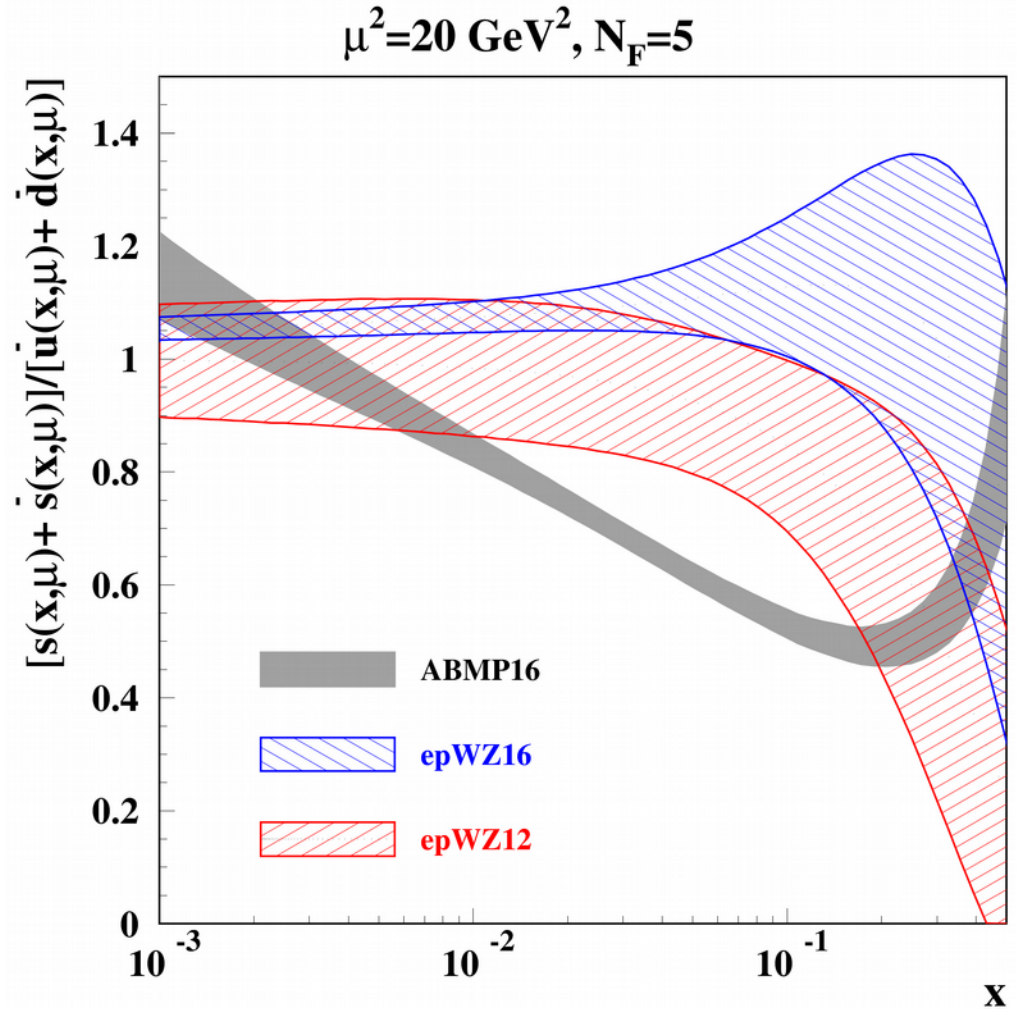
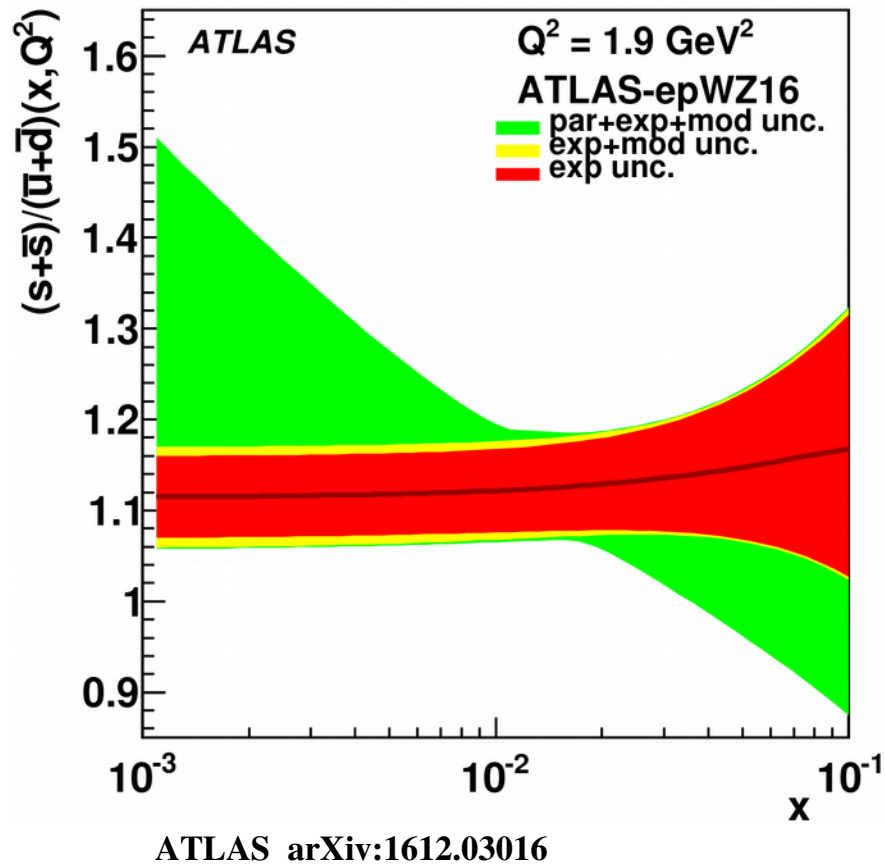
Walker, this conference

Impact of the W-, Z-data



W-, Z-data really control quark disentangling at small x

ATLAS strange enhancement



The epWZ16 strange-sea determined from analysis of the combined HERA-ATLAS data is enhanced as compared to other (earlier) determinations

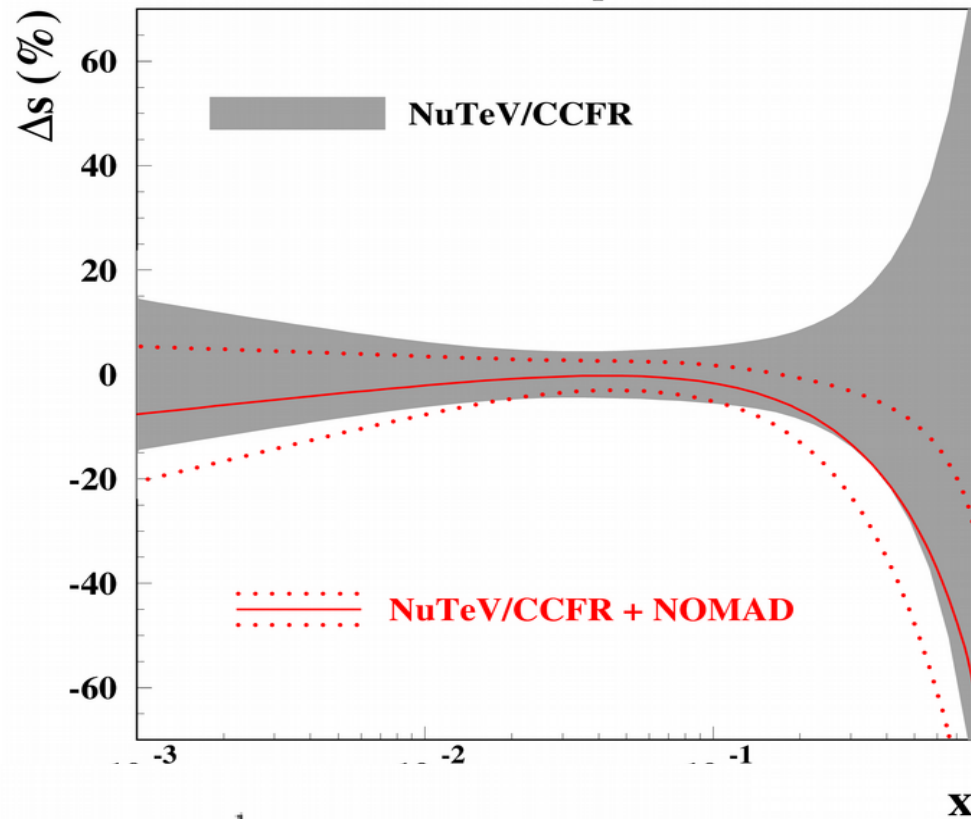
ABM strange sea determination is in particular based on the dimuon neutrino-nucleon DIS production (NuTeV/CCFR and NOMAD) that gives a strange sea suppression ~ 0.5 at $x \sim 0.1$

- *Impact of the nuclear corrections?*
- *Disentangling d- and s- contribution?*
- *.....?*

NOMAD charm data

$\mu=3 \text{ GeV}, n_f=3$

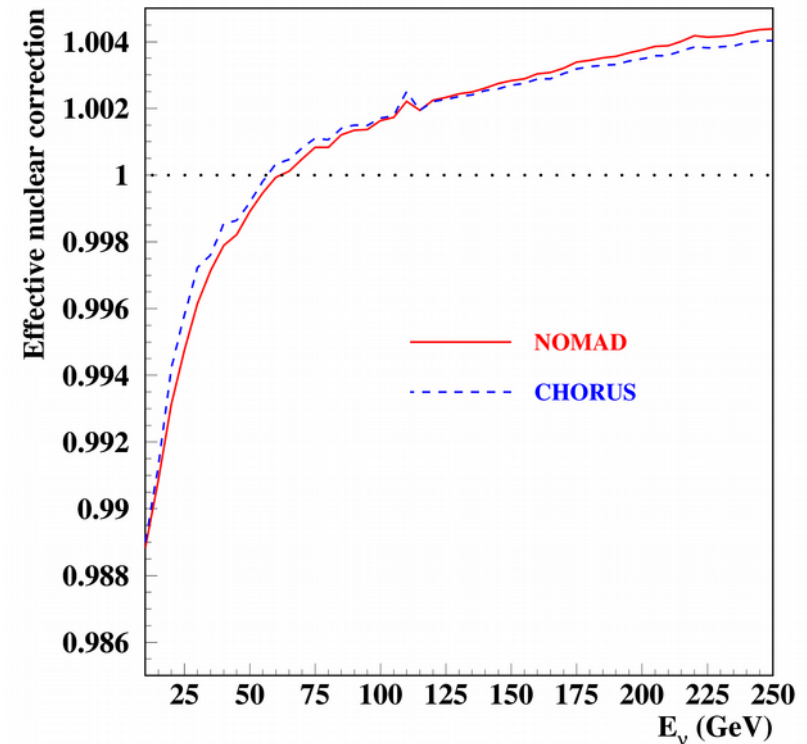
NOMAD NPB 876, 339 (2013)



- The data on ratio $2\mu/\text{incl. CC ratio}$ with the 2μ statistics of 15000 events (much bigger than in earlier CCFR and NuTeV samples).
- Systematics, nuclear corrections, etc. cancel in the ratio
- Pull down strange quarks at $x>0.1$ with a sizable uncertainty reduction

$$\kappa_s(\mu^2) = \frac{\int_0^1 x[s(x, \mu^2) + \bar{s}(x, \mu^2)]dx}{\int_0^1 x[\bar{u}(x, \mu^2) + \bar{d}(x, \mu^2)]dx},$$

Integral suppression factor
 $K_s(20 \text{ GeV}^2)=0.62\pm 0.04$ is obtained

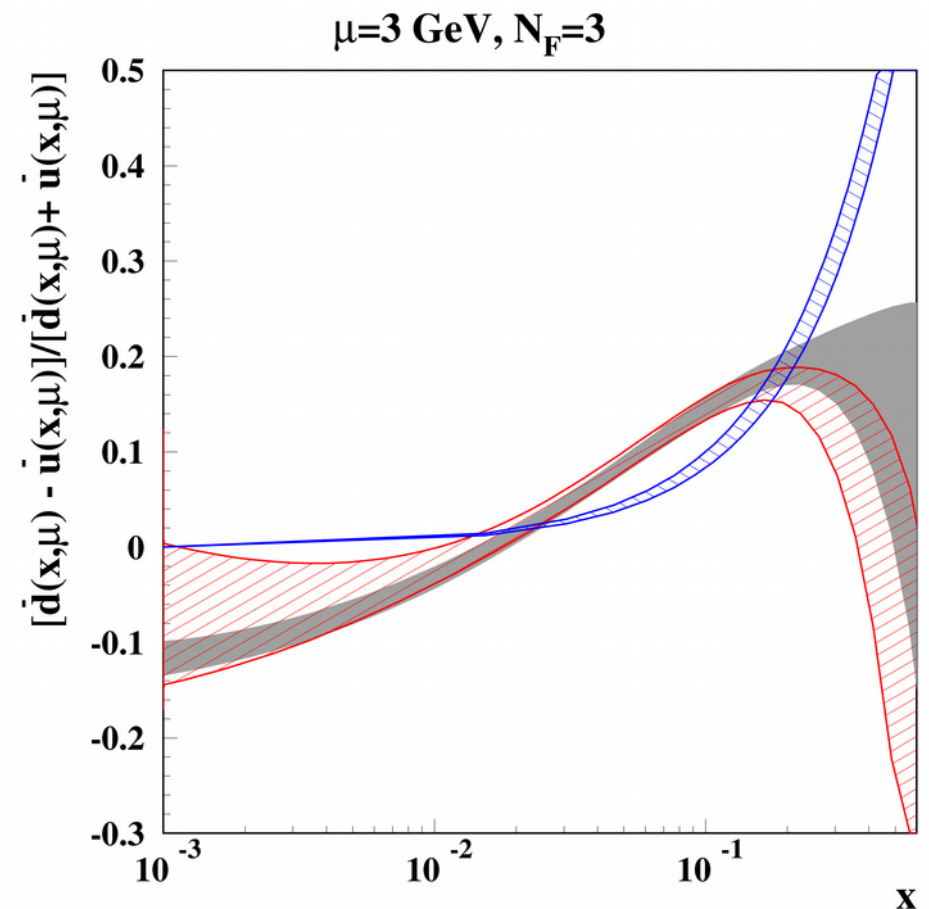
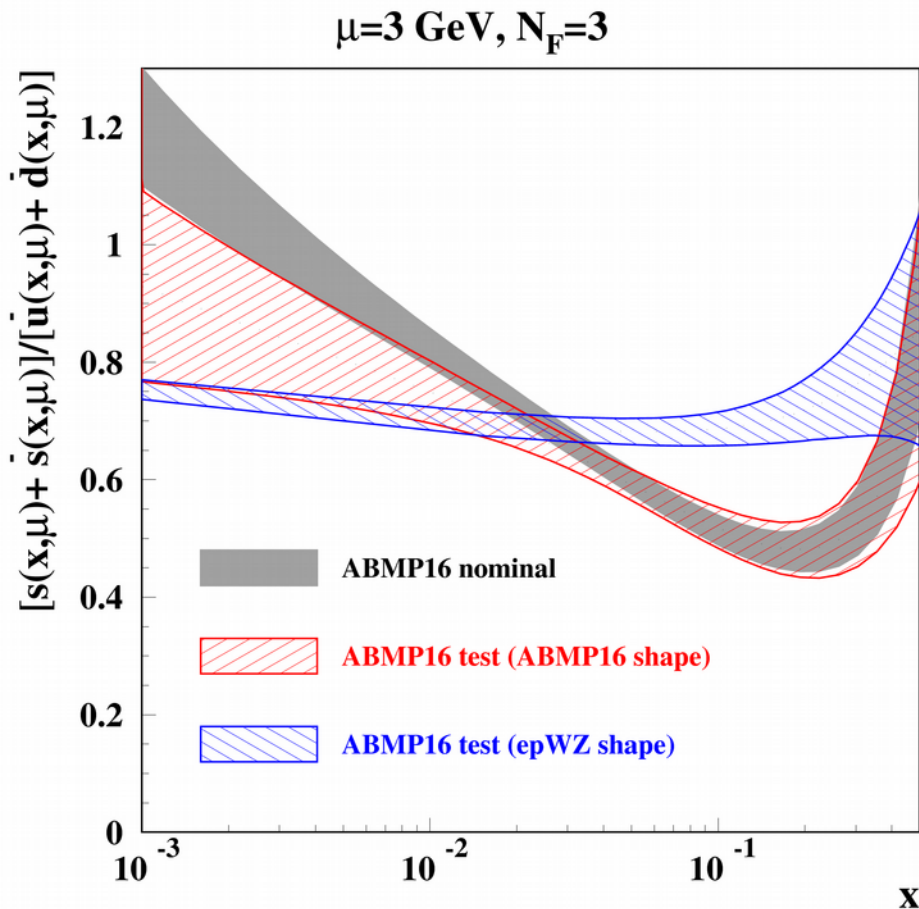


Details of the epWZ and ABMP16 fits

	epWZ16	ABMP16
Data	HERA, ATLAS W&Z	HERA, LHC and Tevatron W&Z, fixed-target DIS and charm production, fixed-target DY,
PDF shape	$xu_v(x, \mu_0^2) = A_{u_v} x^{B_{u_v}} (1-x)^{C_{u_v}} (1 + E_{u_v} x^2),$ $xd_v(x, \mu_0^2) = A_{d_v} x^{B_{d_v}} (1-x)^{C_{d_v}},$ $x\bar{u}(x, \mu_0^2) = A_{\bar{u}} x^{B_{\bar{u}}} (1-x)^{C_{\bar{u}}},$ $x\bar{d}(x, \mu_0^2) = A_{\bar{d}} x^{B_{\bar{d}}} (1-x)^{C_{\bar{d}}},$ $xg(x, \mu_0^2) = A_g x^{B_g} (1-x)^{C_g} - A'_g x^{B'_g} (1-x)^{C'_g},$ $x\bar{s}(x, \mu_0^2) = A_{\bar{s}} x^{B_{\bar{s}}} (1-x)^{C_{\bar{s}}},$ <p style="text-align: center;">15 free parameters</p>	$xq_v(x, \mu_0^2) = \frac{2\delta_{qu} + \delta_{qd}}{N_q^v} (1-x)^{b_{qv}} x^{a_{qv}} P_{qv}(x),$ $xq_s(x, \mu_0^2) = A_{qs} (1-x)^{b_{qs}} x^{a_{qs}} P_{qs}(x),$ $xg(x, \mu_0^2) = A_g (1-x)^{b_g} x^{a_g} P_g(x),$ $P_p(x) = (1 + \gamma_{-1,p} \ln x) \left(1 + \gamma_{1,p} x + \gamma_{2,p} x^2 + \gamma_{3,p} x^3 \right),$ <p style="text-align: center;">25 free parameters</p>

ABMP16 PDFs are selected more flexible in order to accommodate more data as compared to the EpWZ16 fit, which was evolved from the HERA data analysis

Test fit (the PDF shape comparison)

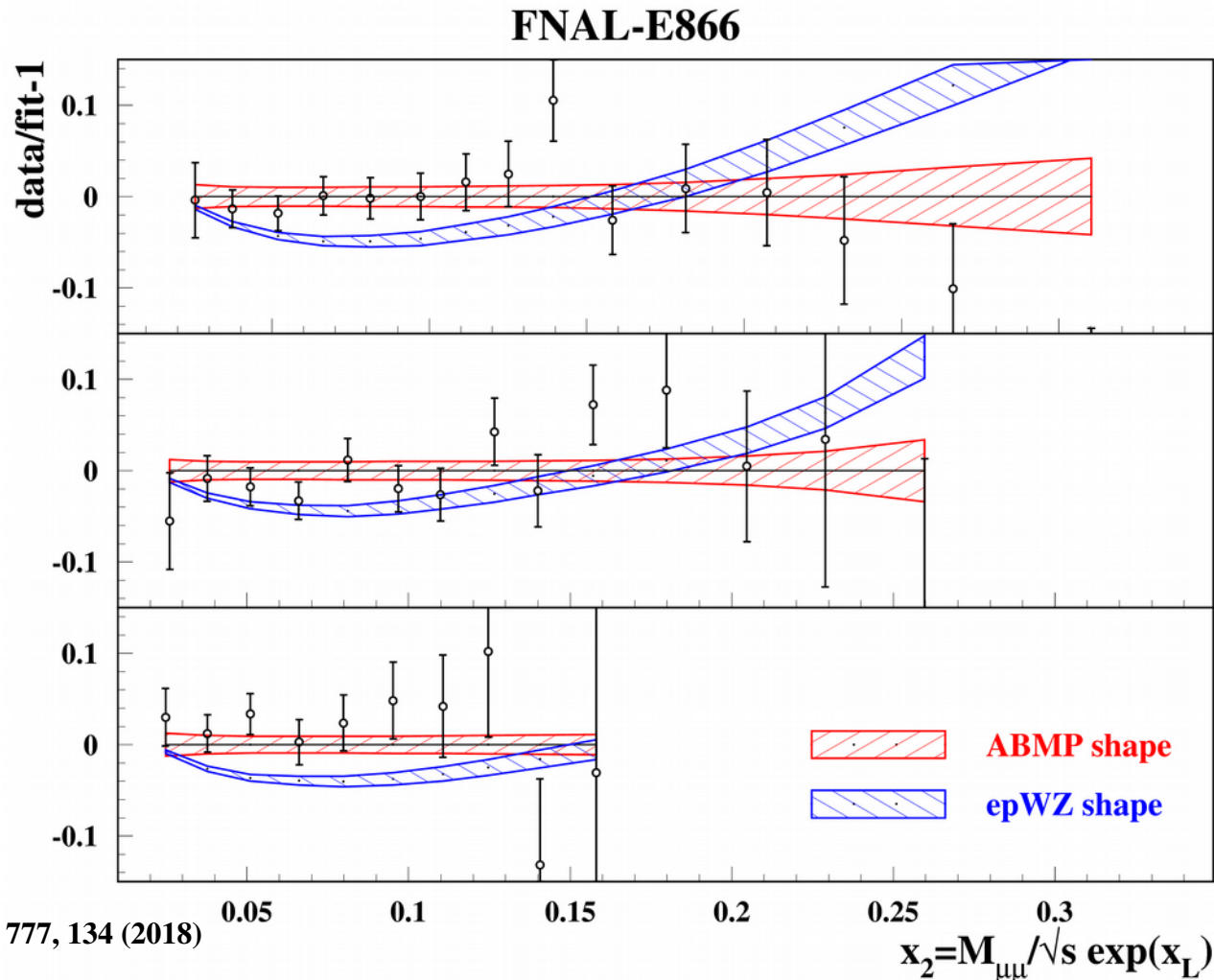


The data used in test fit: collider data discarded and replaced by the deuteron ones
 (fit is consistent with the nominal ABMP16 at $x > 0.01$) sa, Kulagin, Petti hep-ph/1704.00204

The strange sea is enhanced for the epWZ shape despite the ATLAS data are not used. However, the dimuon data description is not deteriorated: $\chi^2=167$ versus 161 for the ABMP shape \Rightarrow enhancement is achieved by the price of the d-quark sea suppression

sa, Blümlein, Caminada, Lipka, Lohwasser,
 Moch, Petti, Plačákytė PRD 91, 094002 (2015)

E866 data in the test fit

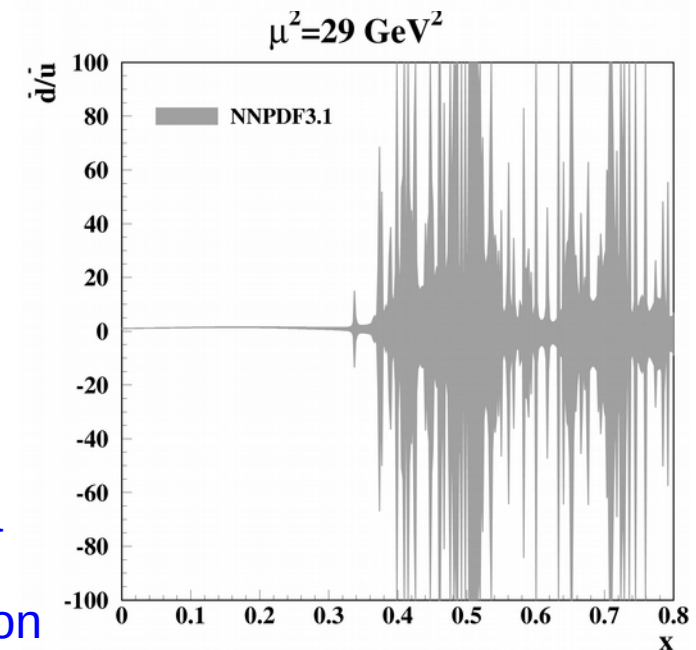
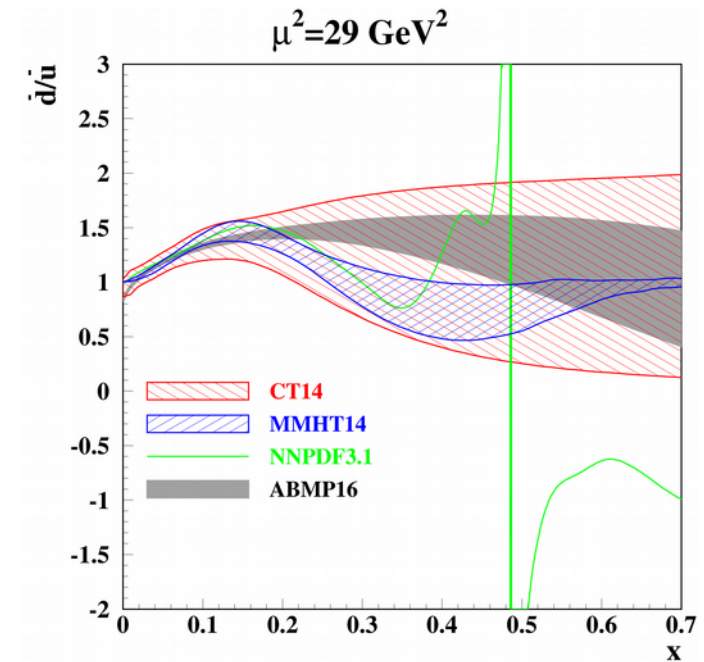
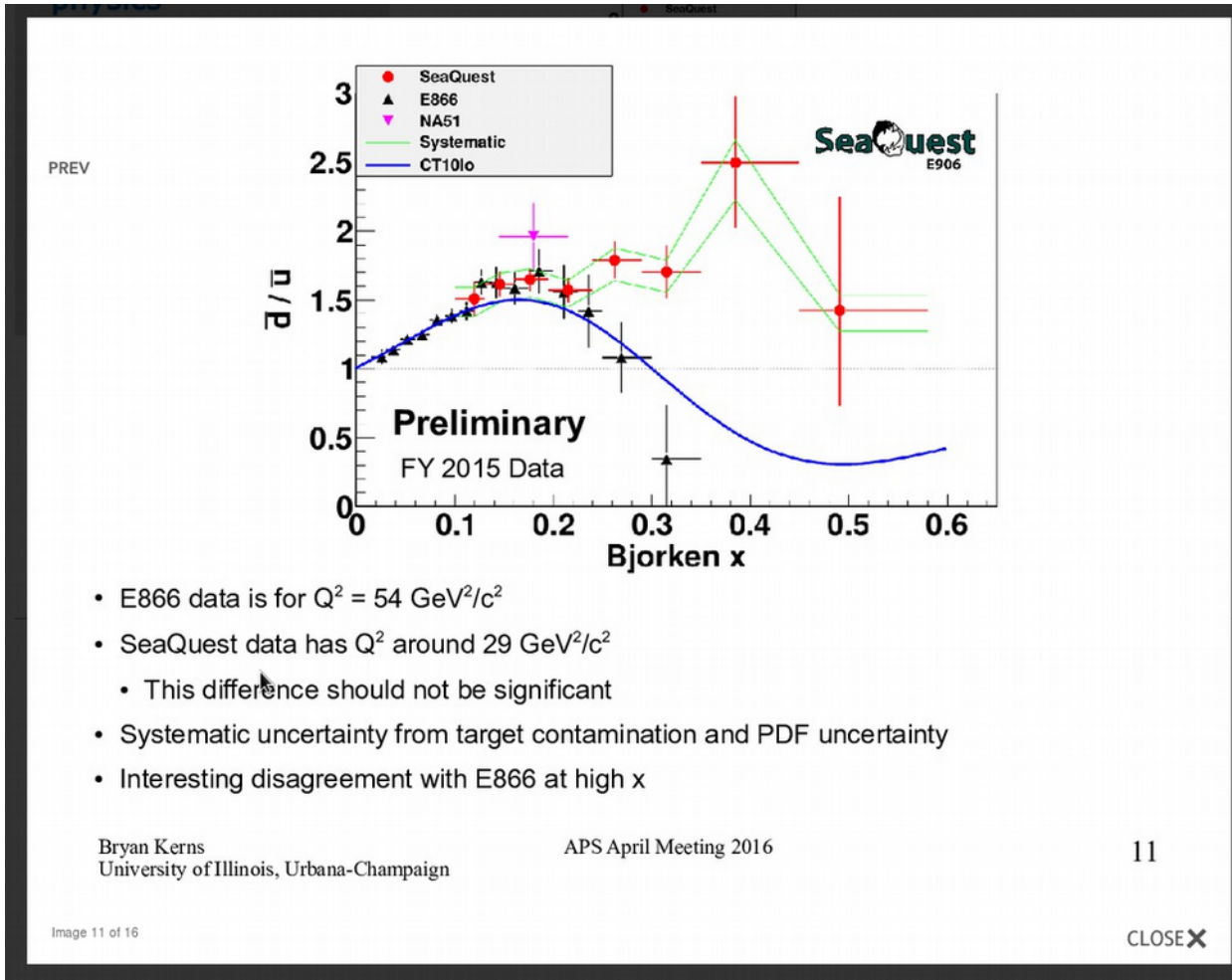


sa, Blümlein, Moch PLB 777, 134 (2018)

The E866 data on p/d DY cross sections are sensitive to the iso-spin sea asymmetry

The epWZ shape does not allow to accommodate E866 data: $\chi^2/NDP=96/39$ versus $49/39$ for the ABMP shape; the errors in epWZ predictions are suppressed at small x , evidently due to over-constrained PDF shape at small x

SeaQuest (FNAL-E906) prospects

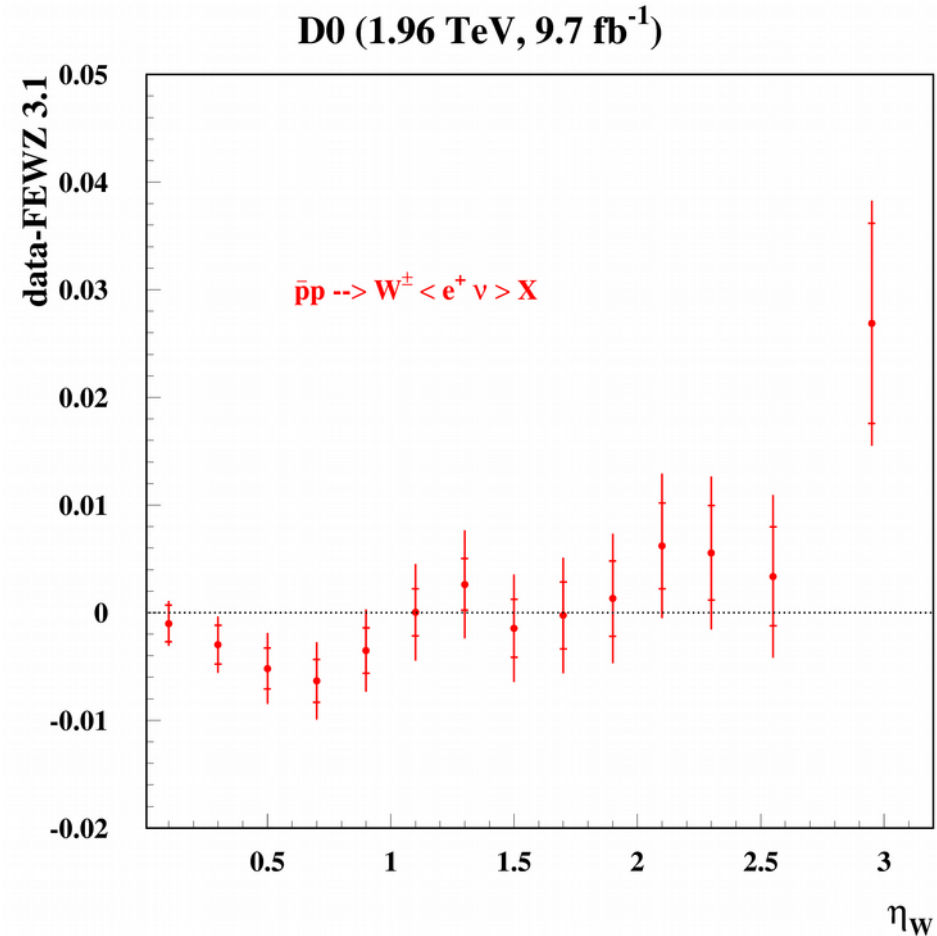
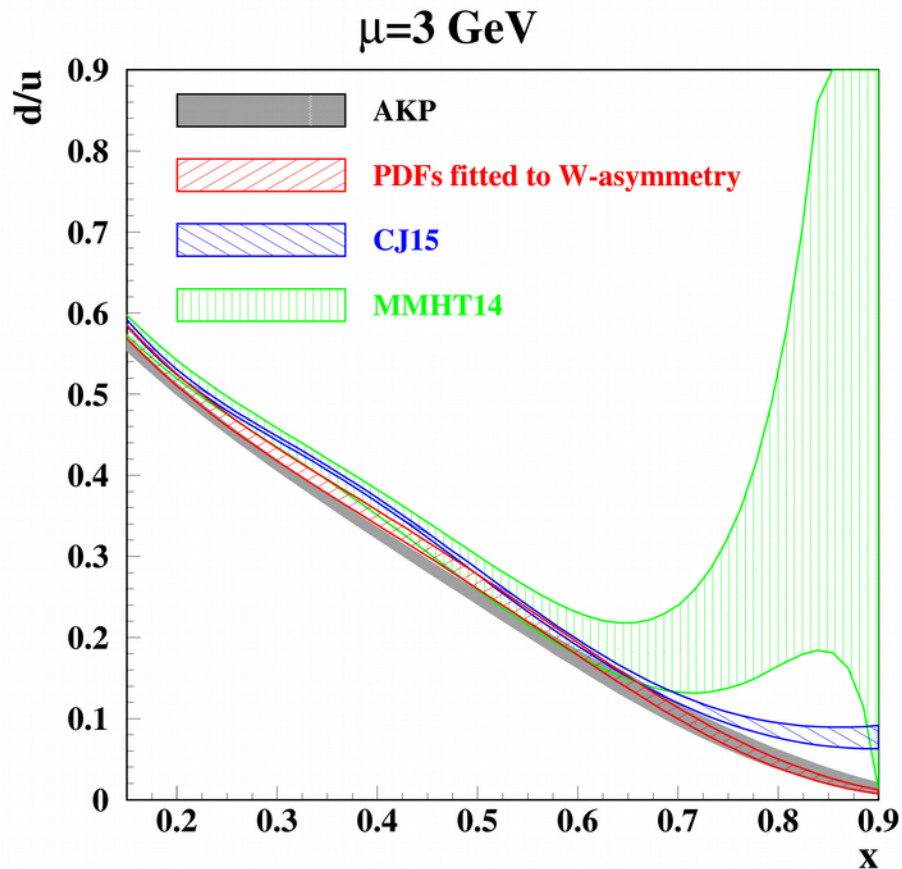


- E906 confirms the E866 results at $x \sim 0.1$ and continues the positive trend in the sea iso-spin asymmetry at larger x
- The existing PDF sets can be consolidated with the E906 data
- HERMES/COMPASS data confirm the strangeness suppression

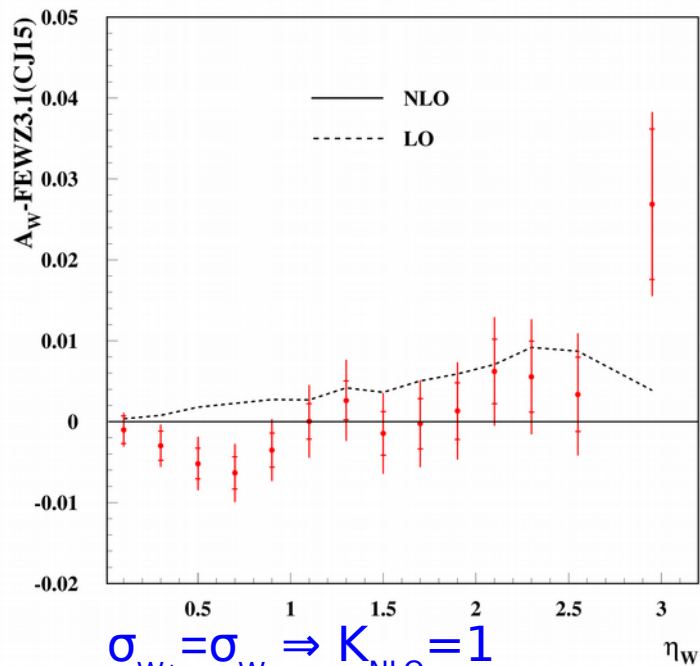
CJ15 results on the d/u ratio

Accardi, Brady, Melnitchouk, Owens, Sato PRD 93, 114017 (2016)

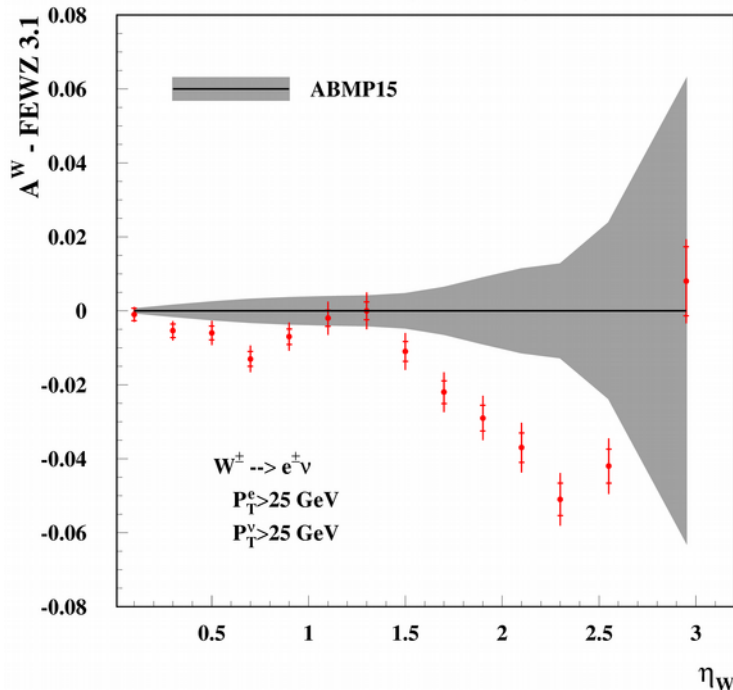
- NLO PDF fit including Tevatron data on W-asymmetry
- value of $d/u \sim 0.07$ at large x is obtained using flexible PDF shape
- FEWZ predictions with CJ15 PDFs miss data at large x ?



D0 (1.96 TeV, 9.7 fb⁻¹)

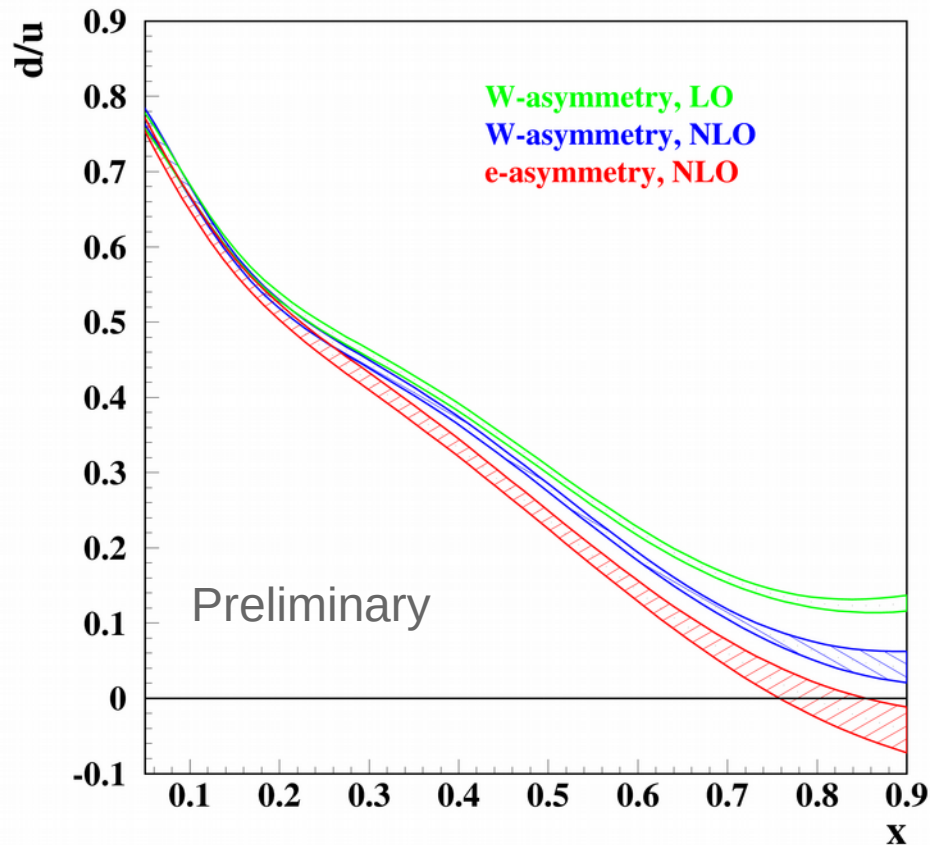


D0 (1.96 TeV, 9.7 fb⁻¹)



W-asymmetry data go lower than predictions based on the e-asymmetry

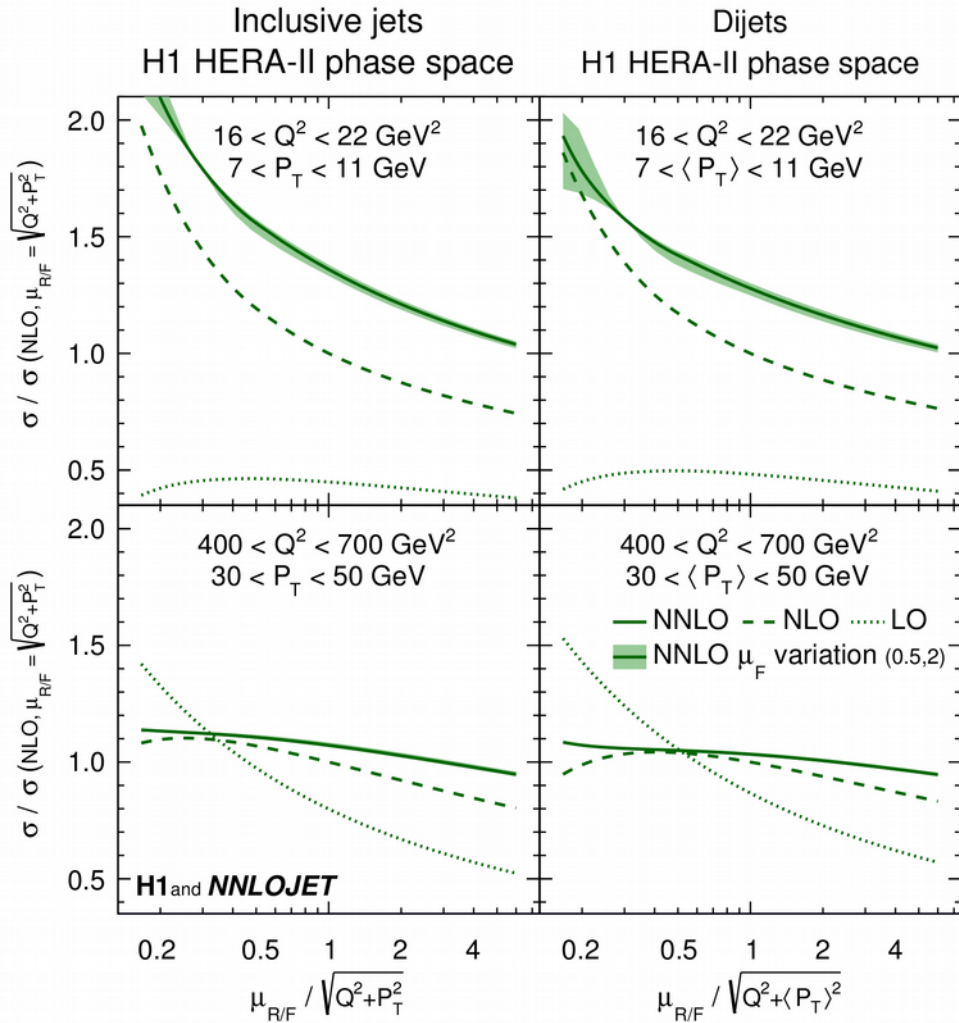
CJ15 shape, $\mu=3 \text{ GeV}$



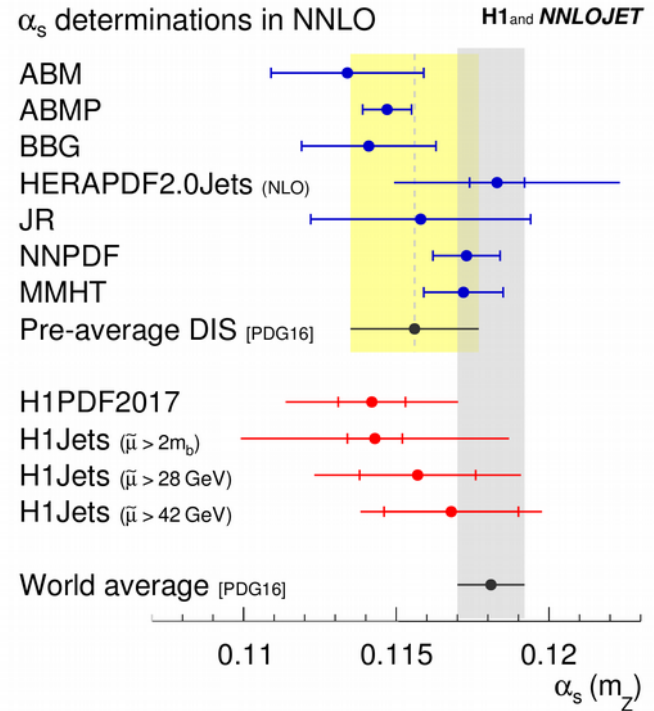
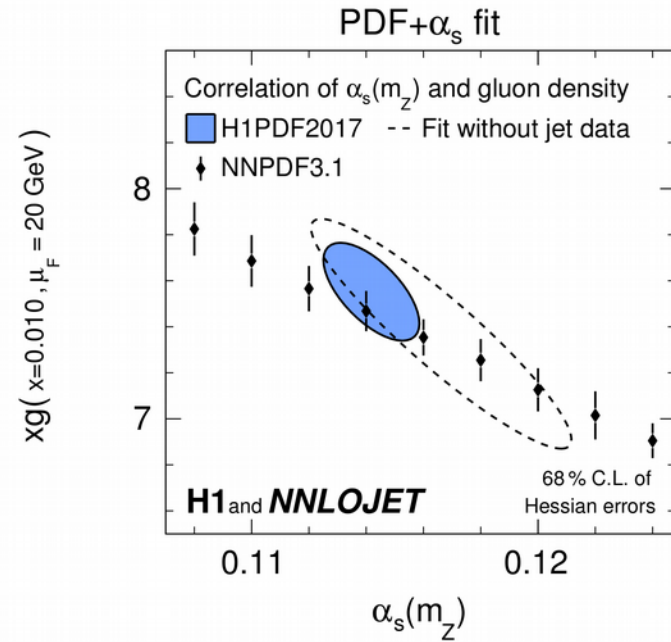
- Account of the NNLO corrections moves large- x d/u downwards
- e-asymmetry data prefer even lower d/u
- agreement with AKP results at large x ; further comparison of deuteron correction is underway

Impact of jets in DIS

H1 EPJC 77, 791 (2017)

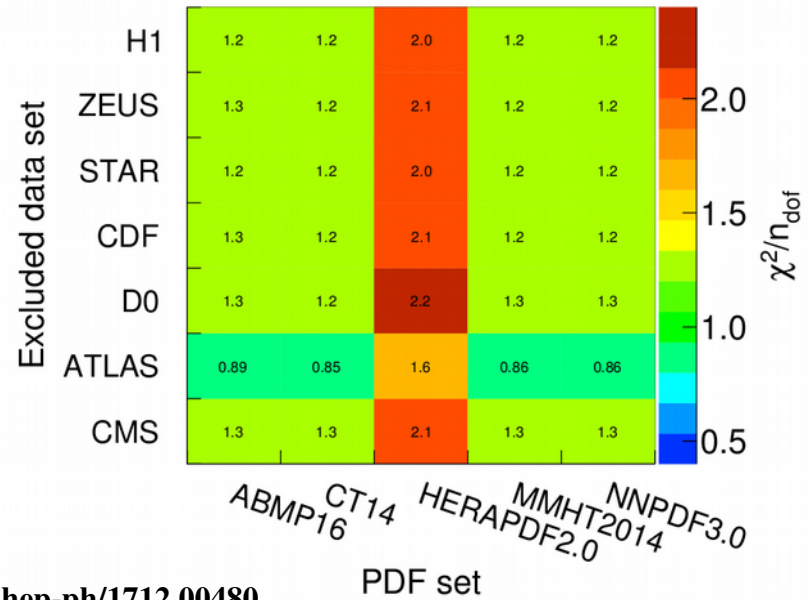
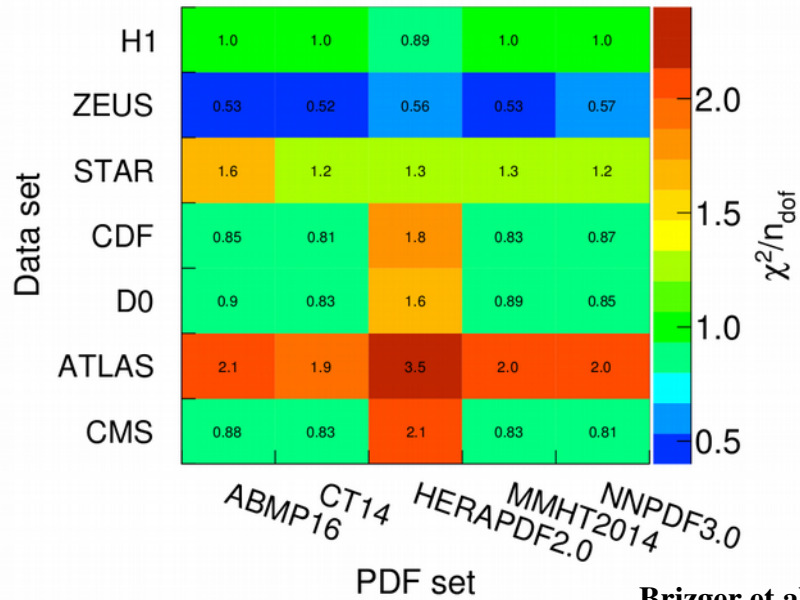


$$\alpha_s(M_Z) = 1142(28) \quad (\text{NNLO})$$



Jets in proton-(anti)proton collisions

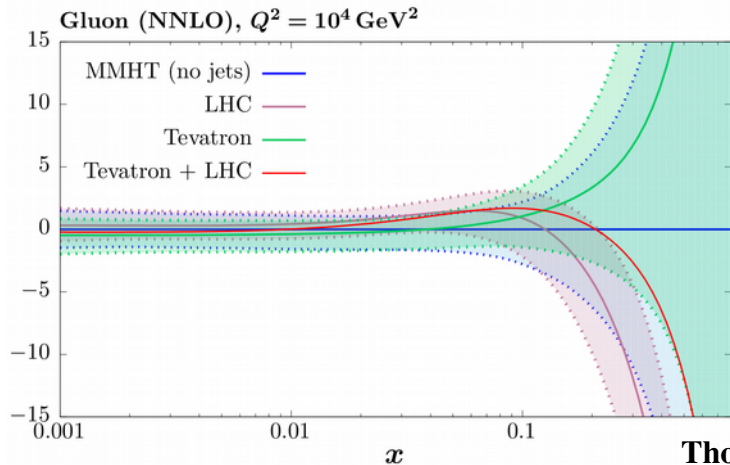
Problem of scale choice: Gehrman-de Ridder, this conference



Brizger et al., hep-ph/1712.00480

	ATLAS	ATLAS, σ_{pd}	ATLAS, σ_{fd}		CMS
$R = 0.4$	350.8 (333.7)	183.1 (170.7)	128.4 (122.2)	$R = 0.5$	191.7 (163.4)
$R = 0.6$	304.0 (264.0)	178.8 (148.9)	128.9 (115.7)	$R = 0.7$	200.1 (175.2)

Error de-correlation reduces χ^2



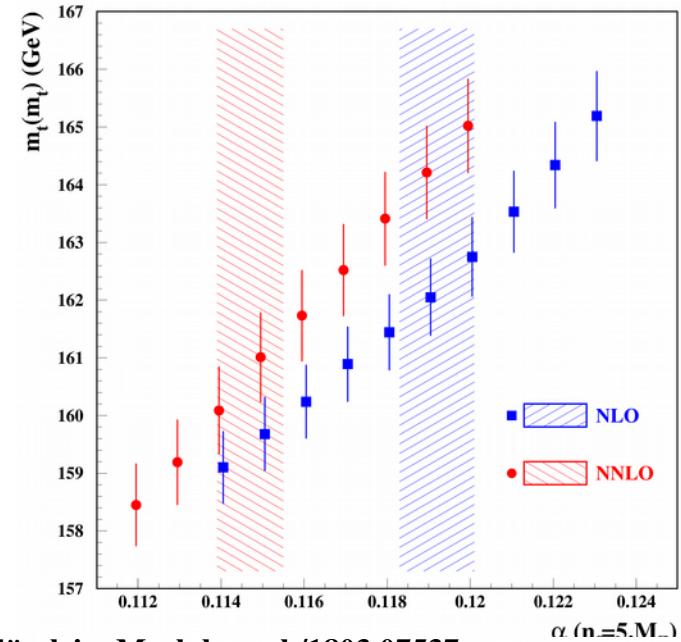
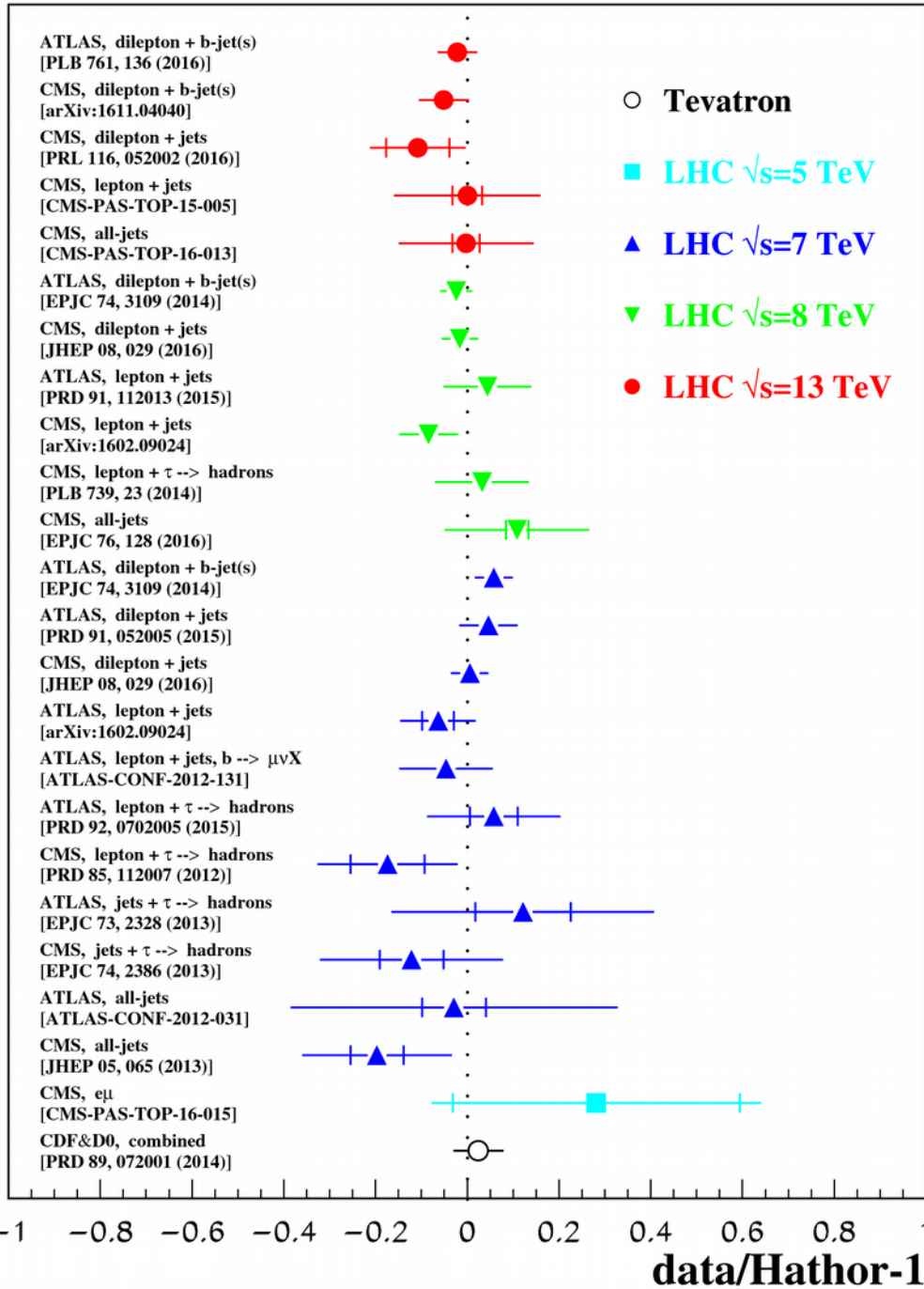
Thorne DIS2018

Jet radius sensitivity: Moch, this conference

Tevatron and LHC data pull gluon in different directions

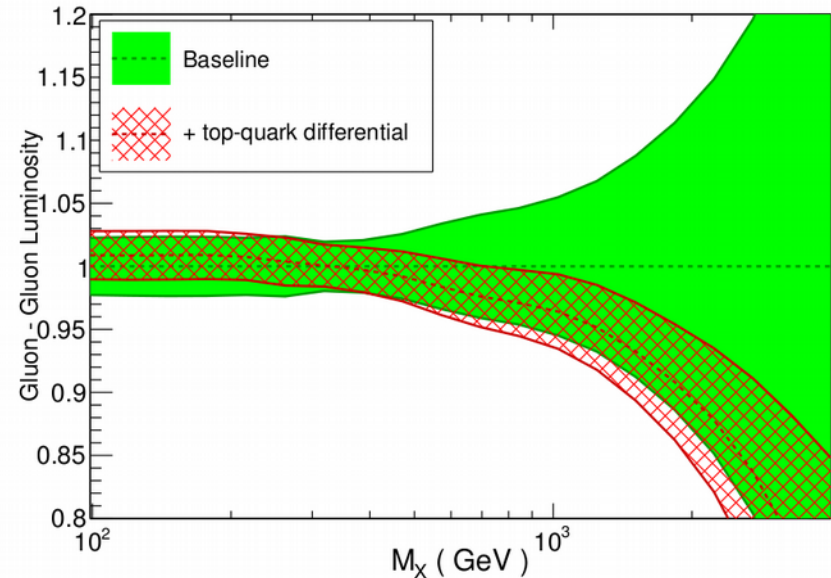
Impact of t-quark data

$\sigma(t\bar{t}X)$



sa, Blümlein, Moch hep-ph/1803.07537

NNLO, global fits, LHC 13 TeV



Czakon et al., JHEP 1704, 044 (2017)

fastNLO

Summary and outlook

- Steady improvement in the quark PDFs' determination due to DY LHC data
 - disentangling d- and u-quark distributions at small x
 - improvement in the large-x d- and u-quark distributions: impact of the forward LHC and Tevatron data; no enhancement in d/u at large x is observed
 - somewhat enhanced strange distribution at small x, however, the large-x enhancement reported by ATLAS seems to be an artifact of the PDF shape used
- The HERA inclusive and semi-inclusive data allow to distinguish between the FFN and VFN factorization schemes in DIS. The FFN scheme provides nice agreement with existing data and

$$m_c(m_c)=1.252\pm 0.018(\text{exp.})-0.01(\text{th.}) \text{ GeV},$$

in a good agreement with other determinations.

- Jet and t-quark data are emerging at NNLO fits due to fast progress of the computational tools.

EXTRAS

The ABMP16 fit ingredients

QCD:

NNLO evolution

NNLO massless DIS and DY coefficient functions

NLO+ massive DIS coefficient functions (**FFN scheme**)

– NLO + NNLO(approx.) corrections for NC

– NNLO CC at $Q \gg m_c$

– running mass

NNLO exclusive DY (FEWZ 3.1)

NNLO inclusive $t\bar{t}$ production (pole / running mass)

Relaxed form of $(d\bar{u}-u\bar{d})$ at small x

DATA:

DIS NC/CC inclusive (HERA I+II added)

DIS NC charm production (HERA)

DIS CC charm production (HERA, NOMAD, CHORUS, NuTeV/CCFR)

fixed-target DY

LHC DY distributions (ATLAS, CMS, LHCb)

t -quark data from the LHC and Tevatron

Power corrections:

target mass effects

dynamical twist-4 terms

sa, Blümlein, Moch, Plačákyté PRD 96, 014011 (2017)

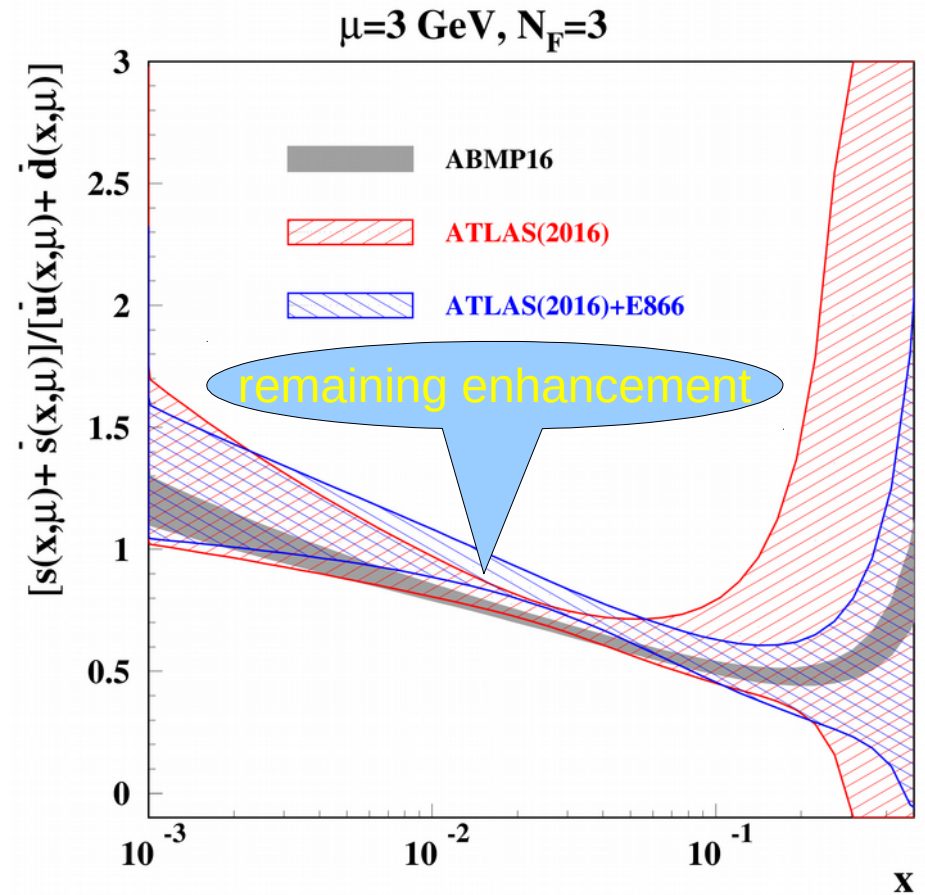
.....

Impact of ATLAS data with flexible PDF shape

	$\kappa_s(\mu^2=20 \text{ GeV}^2)$
HERA+ATLAS	0.81(18)
HERA+ATLAS+E866	0.72(8)
ABMP16(incl. NOMAD)	0.66(3)

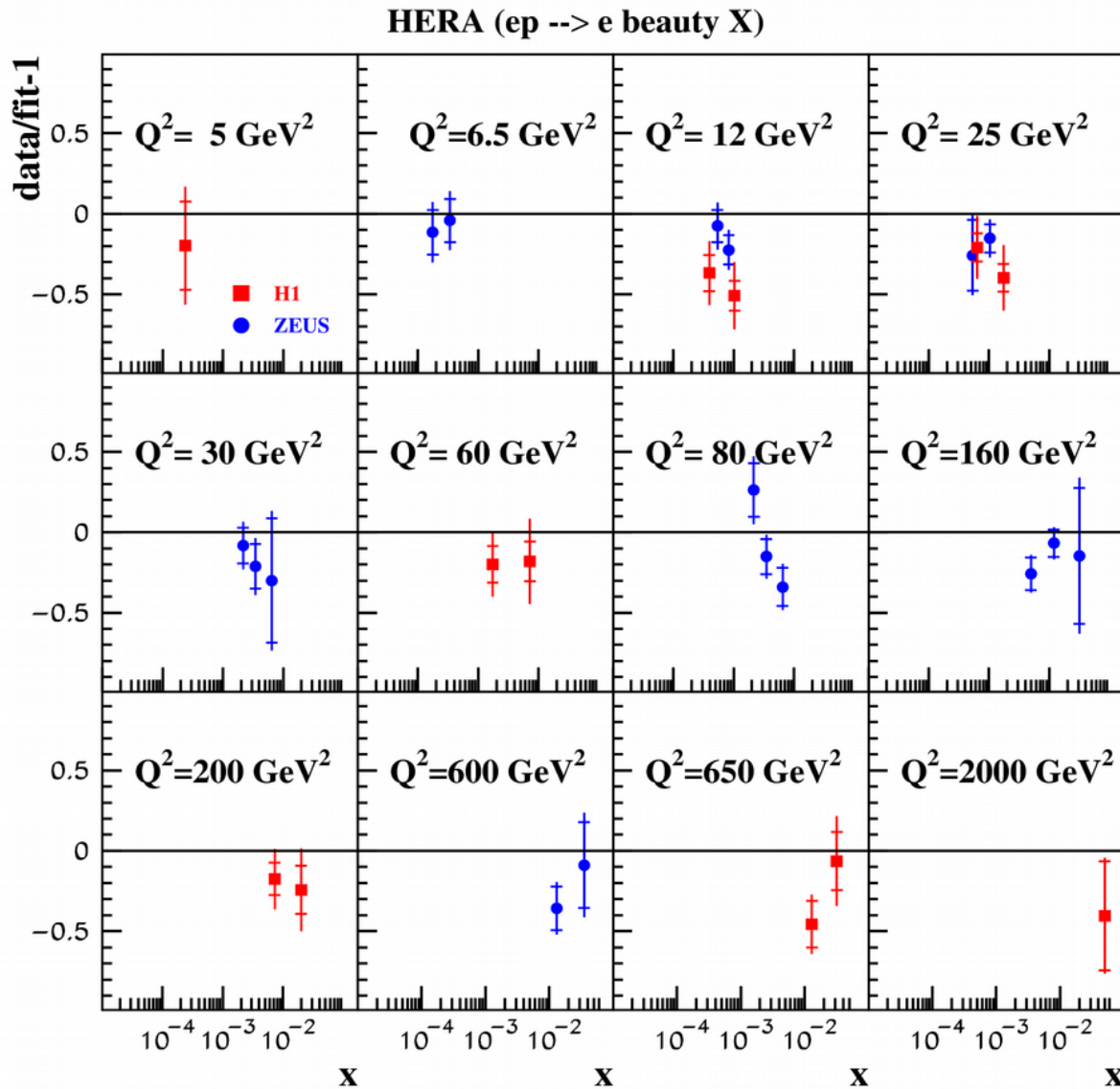
κ_s is integral strange sea suppression factor:

$$\kappa_s(\mu^2) = \frac{\int_0^1 x[s(x, \mu^2) + \bar{s}(x, \mu^2)]dx}{\int_0^1 x[\bar{u}(x, \mu^2) + \bar{d}(x, \mu^2)]dx},$$



- For the flexible PDF shape the strangeness is in a broad agreement with the one extracted from the dimuon data
- The E866 data are consistent with the ATLAS(2016) set: $\chi^2/\text{NDP}=48/39$ and $40/34$, respectively.

HERA bottom data and $m_b(m_b)$



ZEUS JHEP 1409, 127 (2014)

$$\chi^2/\text{NDP} = 16/17$$

H1 EPJC 65, 89 (2010)

$$\chi^2/\text{NDP} = 5/12$$

$$m_b(m_b) = 3.83 \pm 0.12(\text{exp.}) - 0.1(\text{th.}) \text{ GeV}$$

NNLO DY corrections in the fit

The existing NNLO codes (DYNNLO, FEWZ) are quite time-consuming → fast tools are employed (FASTNLO, Applgrid,.....)

- the corrections for certain basis of PDFs are stored in the grid
- the fitted PDFs are expanded over the basis
- the NNLO c.s. in the PDF fit is calculated as a combination of expansion coefficients with the pre-prepared grids

The general PDF basis is not necessary since the PDFs are already constrained by the data, which do not require involved computations → *use as a PDF basis the eigenvalue PDF sets obtained in the earlier version of the fit*

$\mathbf{P}_0 \pm \Delta\mathbf{P}_0$ – vector of PDF parameters with errors obtained in the earlier fit

\mathbf{E} – error matrix

\mathbf{P} – current value of the PDF parameters in the fit

- store the DY NNLO c.s. for all PDF sets defined by the eigenvectors of \mathbf{E}
- the variation of the fitted PDF parameters ($\mathbf{P} - \mathbf{P}_0$) is transformed into this eigenvector basis
- the NNLO c.s. in the PDF fit is calculated as a combination of transformed ($\mathbf{P} - \mathbf{P}_0$) with the stored eigenvector values

PDF sets	m_c [GeV]	m_c renorm. scheme	theory method (F_2^c scheme)	theory accuracy for heavy quark DIS Wilson coeff.	χ^2 /NDP for HERA data [127] with xFitter [128, 129]	
ABM12 [2] ^a	$1.24^{+0.05}_{-0.03}$	$\overline{\text{MS}}$ $m_c(m_c)$	FFNS ($n_f = 3$)	NNLO _{approx}	65/52	66/52
CJ15 [1]	1.3	m_c^{pole}	SACOT [122]	NLO	117/52	117/52
CT14 [3] ^b						
(NLO)	1.3	m_c^{pole}	SACOT(χ) [123]	NLO	51/47	70/47
(NNLO)	1.3	m_c^{pole}	SACOT(χ) [123]	NLO	64/47	130/47
HERAPDF2.0 [4]						
(NLO)	1.47	m_c^{pole}	RT optimal [125]	NLO	67/52	67/52
(NNLO)	1.43	m_c^{pole}	RT optimal [125]	NLO	62/52	62/52
JR14 [5] ^c	1.3	$\overline{\text{MS}}$ $m_c(m_c)$	FFNS ($n_f = 3$)	NNLO _{approx}	62/52	62/52
MMHT 14 [6]						
(NLO)	1.4	m_c^{pole}	RT optimal [125]	NLO	72/52	78/52
(NNLO)	1.4	m_c^{pole}	RT optimal [125]	NLO	71/52	83/52
NNPDF3.0 [7]						
(NLO)	1.275	m_c^{pole}	FONLL-B [124]	NLO	58/52	60/52
(NNLO)	1.275	m_c^{pole}	FONLL-C [124]	NLO	67/52	69/52
PDF4LHC15 [8] ^d	–	–	FONLL-B [124]	–	58/52	64/52
	–	–	RT optimal [125]	–	71/52	75/52
	–	–	SACOT(χ) [123]	–	51/47	76/47

No advantage of the GMVFN schemes: the VFN χ^2 values are systematically bigger than the FFN ones

Accardi, et al. hep-ph/1603.08906

Charm quark mass and the Higgs cross section

MMHT

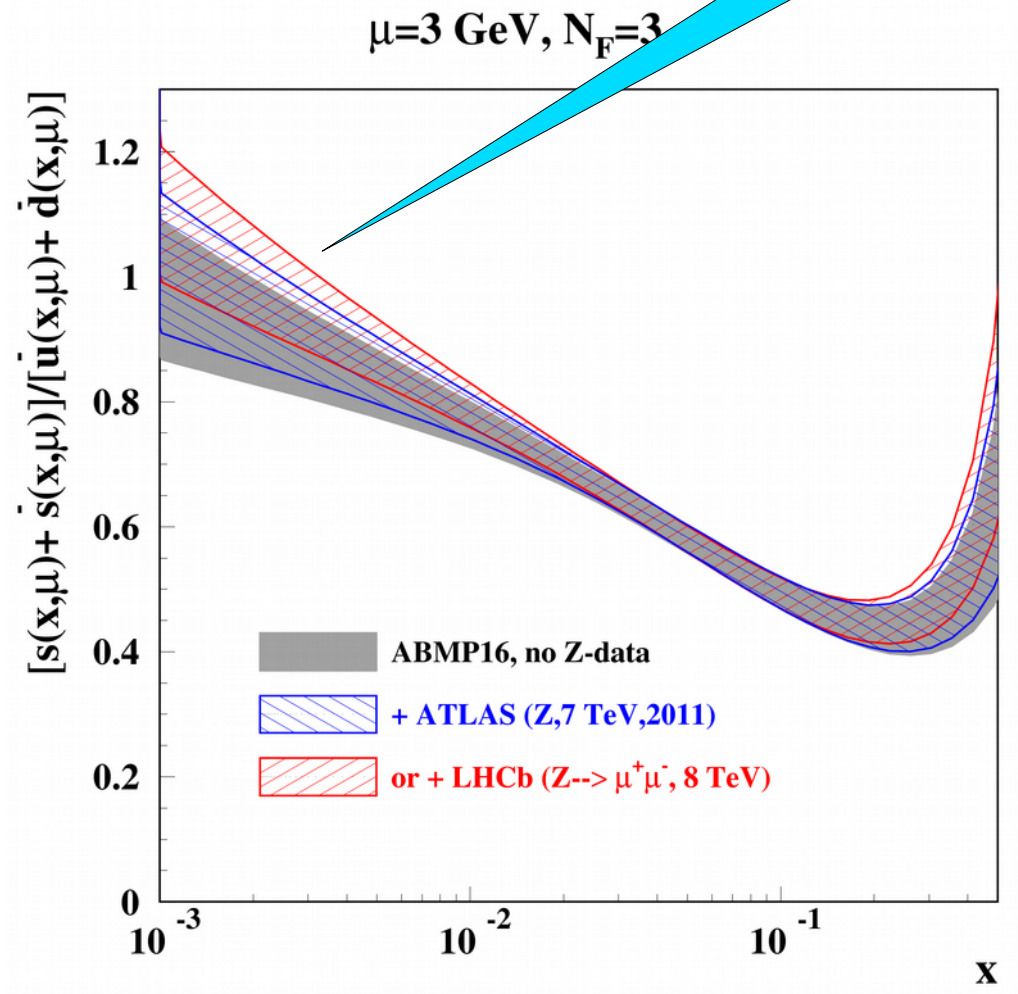
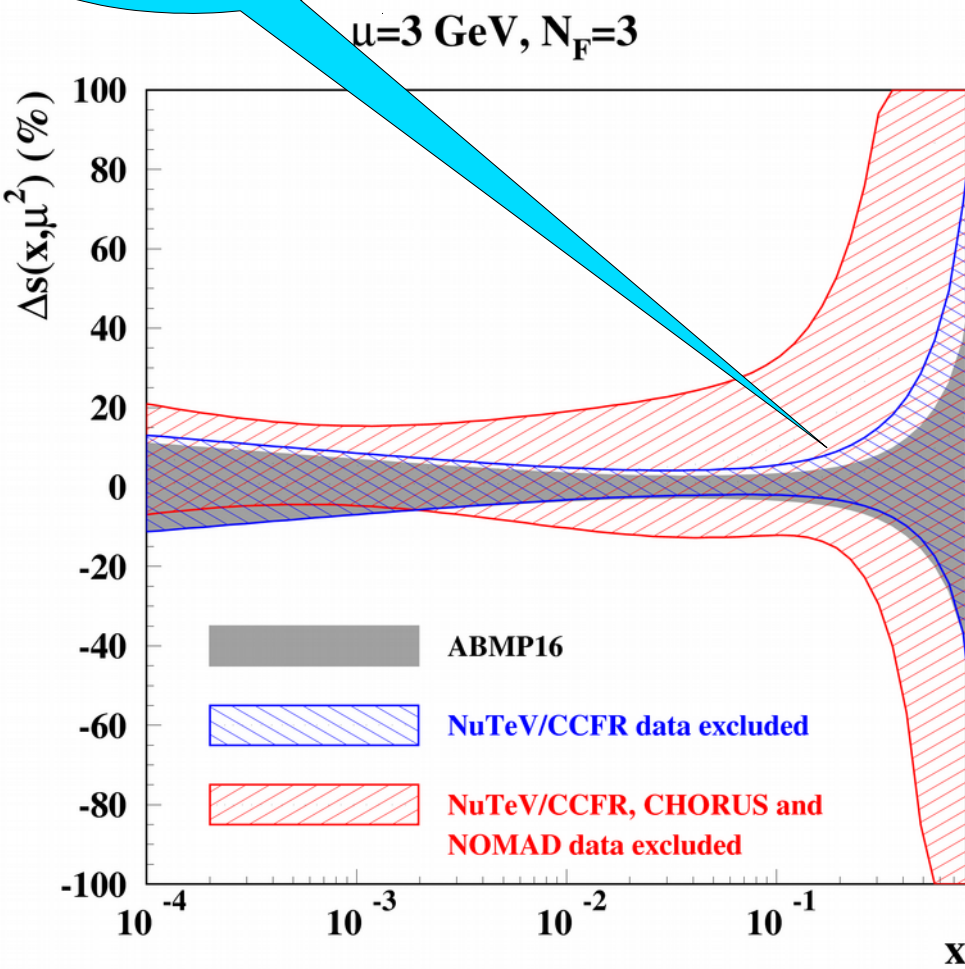
- “Tuning” Charm mass m_c parameter effects the Higgs cross section
 - linear rise in $\sigma(H) = 40.5 \dots 42.6$ pb for $m_c = 1.15 \dots 1.55$ GeV with MMHT14 PDFs [Martin, Motylinski, Harland-Lang, Thorne '15](#)

m_c^{pole} [GeV]	$\alpha_s(M_Z)$ (best fit)	χ^2/NDP (HERA data on $\sigma^{c\bar{c}}$)	$\sigma(H)^{\text{NNLO}}$ [pb] best fit $\alpha_s(M_Z)$	$\sigma(H)^{\text{NNLO}}$ [pb] $\alpha_s(M_Z) = 0.118$
1.15	0.1164	78/52	40.48	(42.05)
1.2	0.1166	76/52	40.74	(42.11)
1.25	0.1167	75/52	40.89	(42.17)
1.3	0.1169	76/52	41.16	(42.25)
1.35	0.1171	78/52	41.41	(42.30)
1.4	0.1172	82/52	41.56	(42.36)
1.45	0.1173	88/52	41.75	(42.45)
1.5	0.1173	96/52	41.81	(42.51)
1.55	0.1175	105/52	42.08	(42.58)

Constraints on strange sea

Controlled by
NOMAD

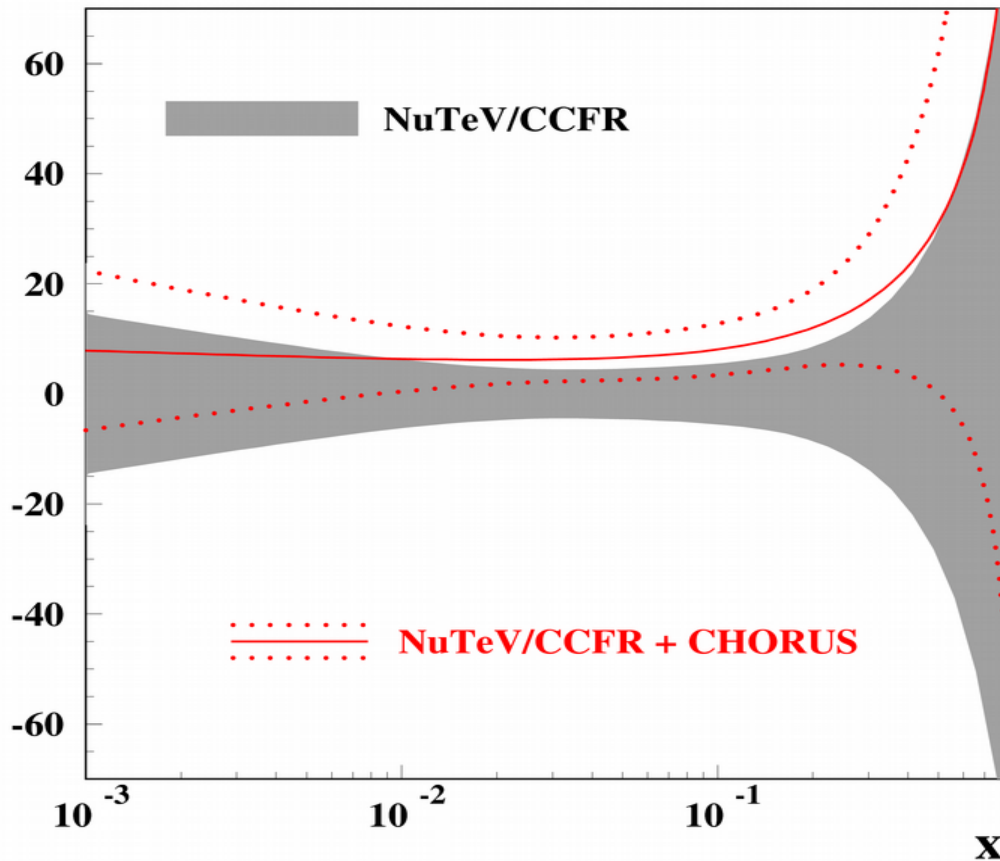
Controlled by
DY&DIS(incl.)



- Uncertainty of $\sim 5\%$ is achieved at x around 0.1
- NuTeV/CCFR data play no essential role \rightarrow impact of the nuclear corrections is greatly reduced (NOMAD and CHORUS give the ratio CC/incl.)

CHORUS charm data

$\mu=3 \text{ GeV}, n_f=3$



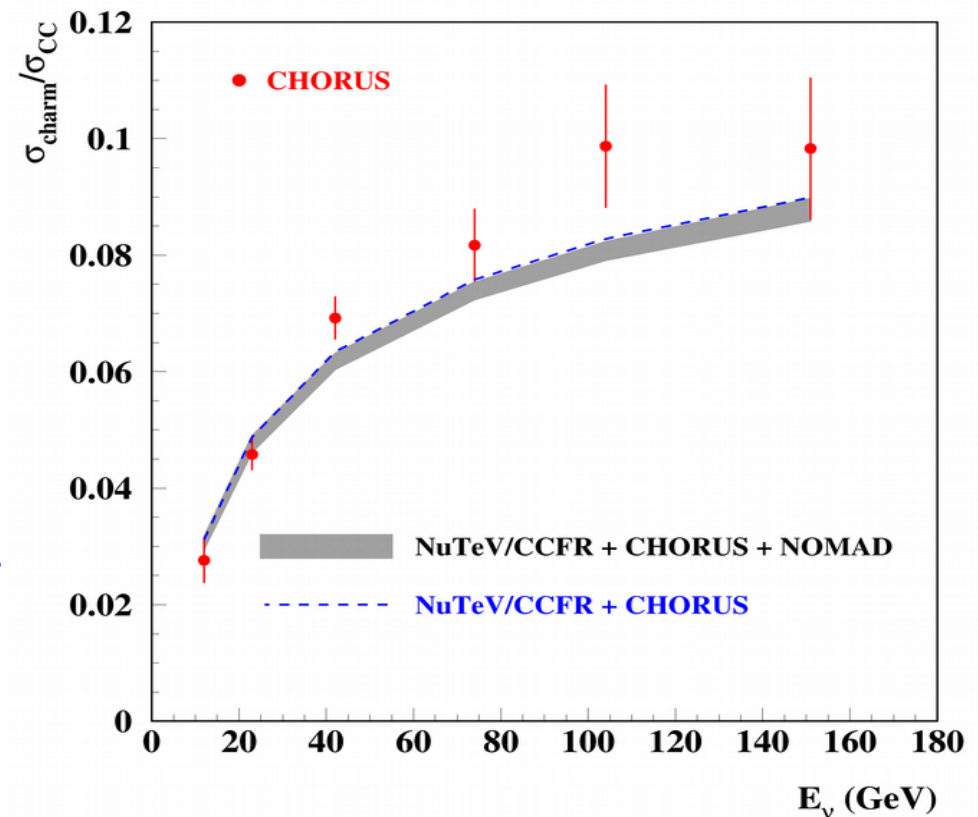
CHORUS data pull strangeness up, however the statistical significance of the effect is poor

sa, Blümlein, Caminada, Lipka, Lohwasser, Moch, Petti, Placakyte hep-ph/1404.6469

Emulsion data on charm/CC ratio with the charmed hadron vertex measured

CHORUS NJP 13, 093002 (2011)

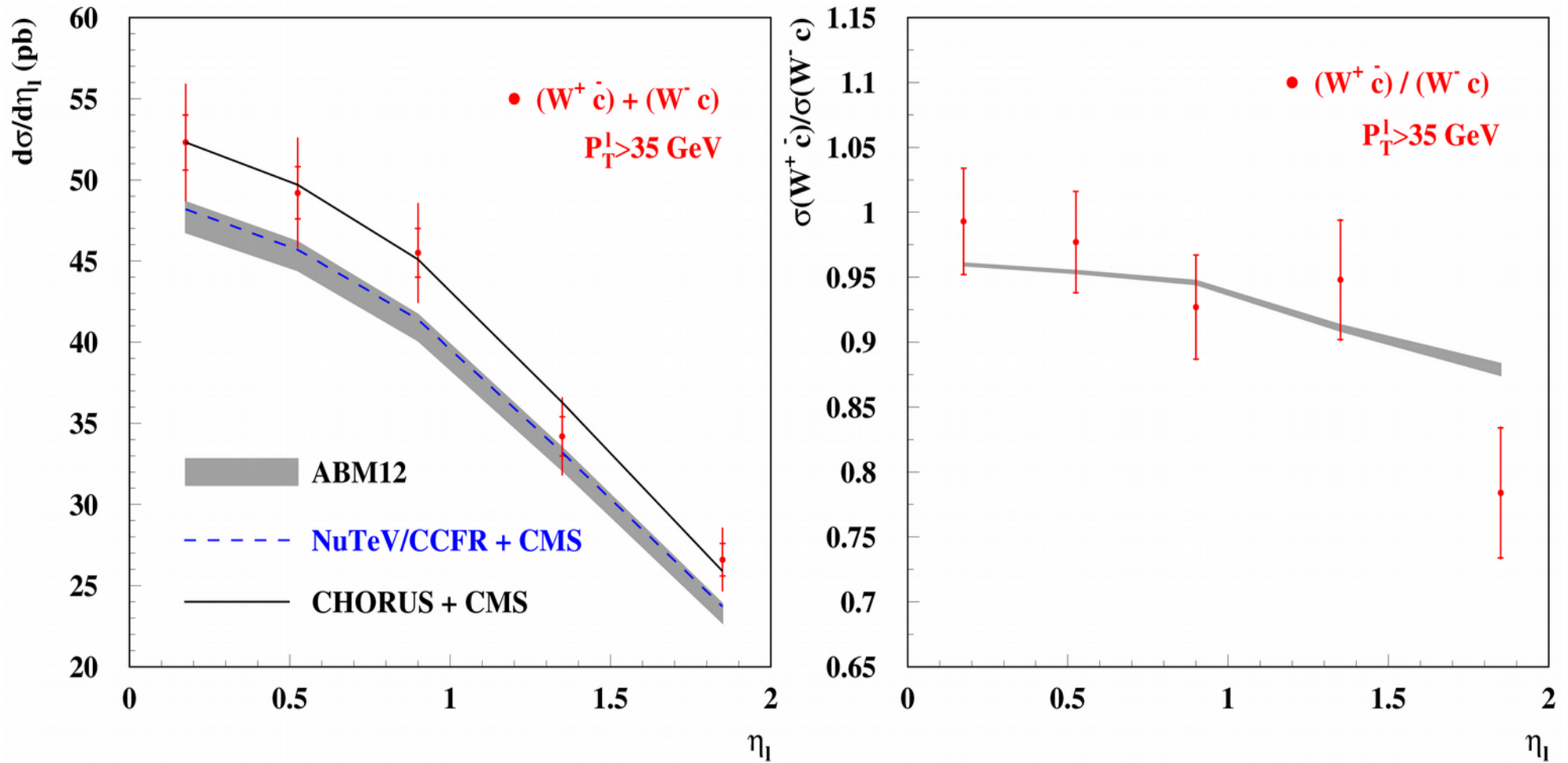
- full phase space measurements
- no sensitivity to B_μ
- low statistics (2013 events)



CMS W+charm data

CMS Collaboration JHEP 02, 013 (2014)

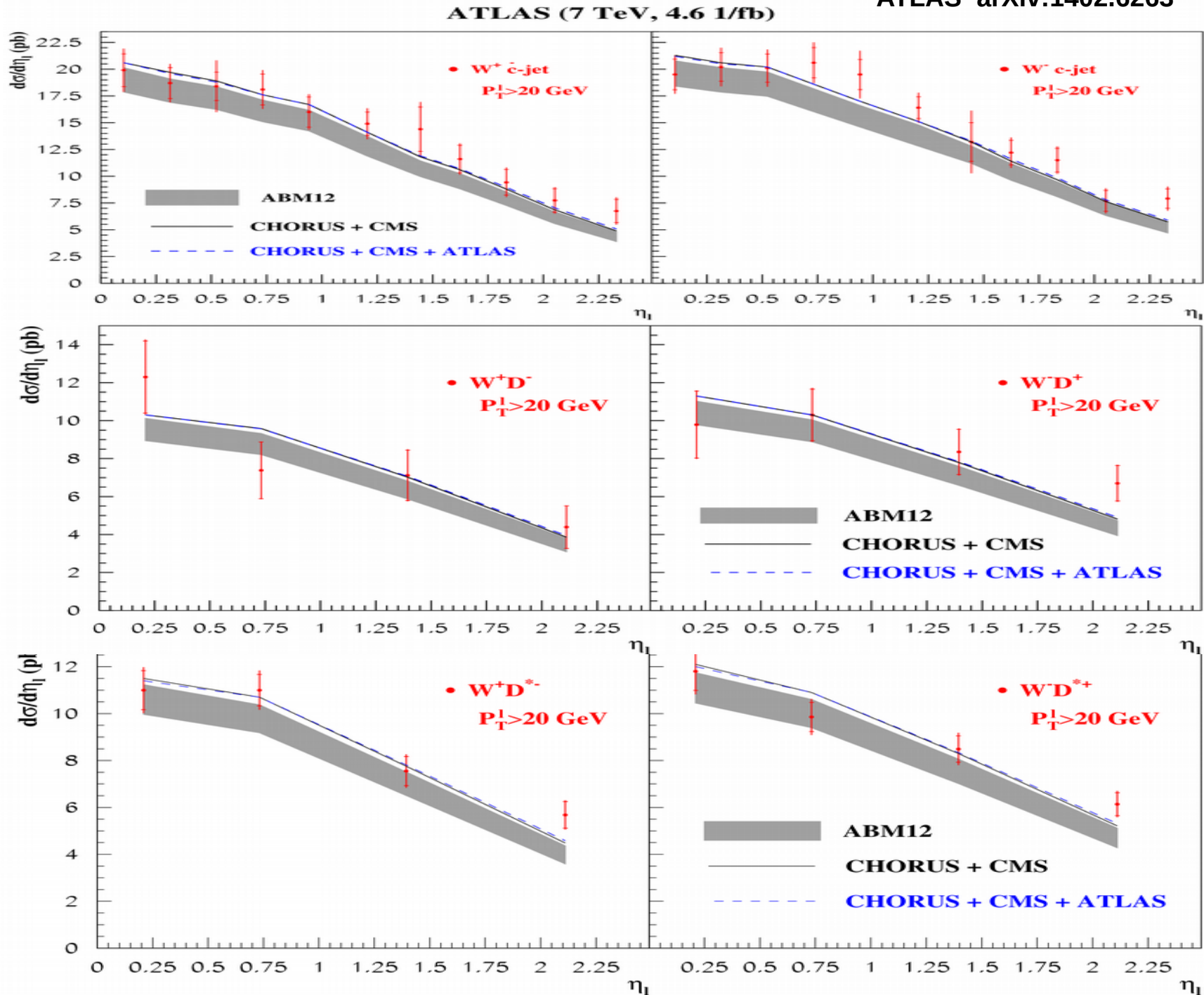
CMS (7 TeV, 5 1/fb)



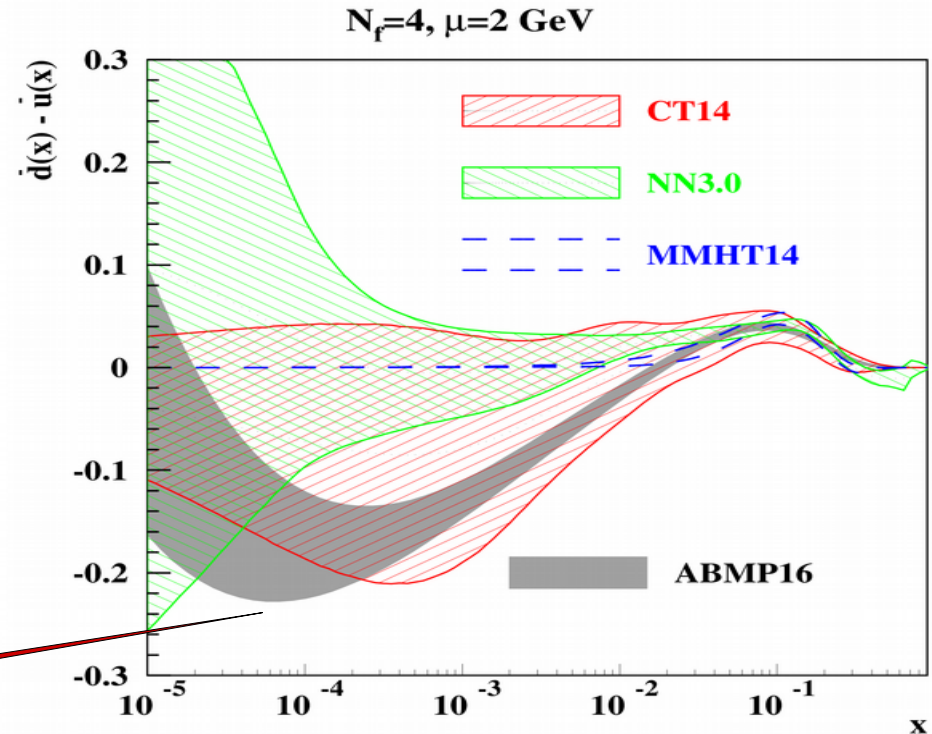
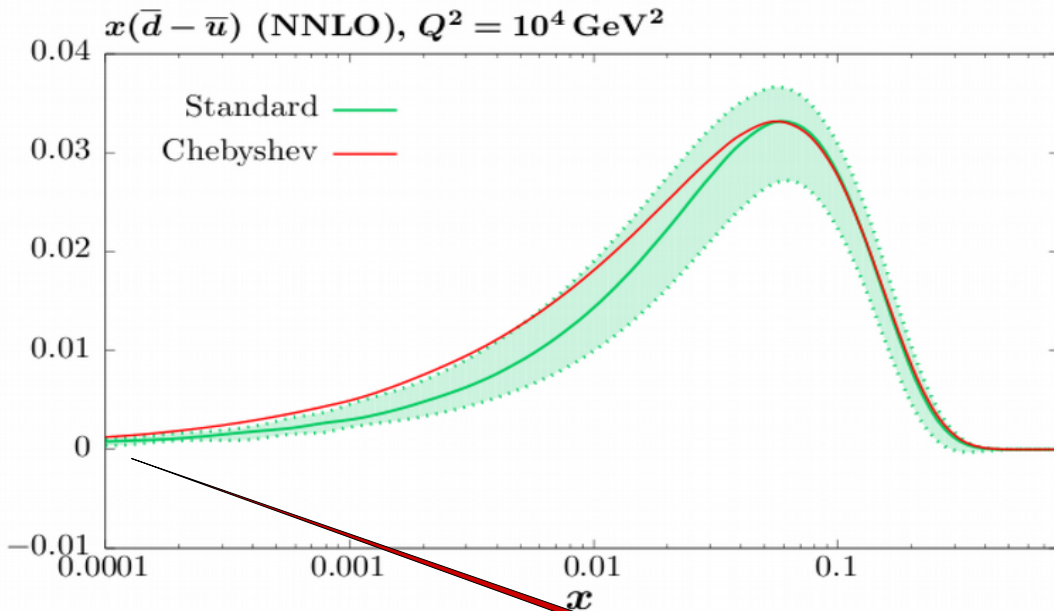
- CMS data go above the NuTeV/CCFR by 1σ ; little impact on the strange sea
- The charge asymmetry is in a good agreement with the charge-symmetric strange sea
- Good agreement with the CHORUS data

ATLAS W+charm data

ATLAS arXiv:1402.6263



$$(\bar{d} - \bar{u})(x, Q_0^2) = A(1 - x)^{\eta_{sea} + 2} x^\delta (1 + \sum_{i=1}^4 a_i T_i(1 - 2x^{\frac{1}{2}})),$$



Thorne, this conference

	no. points	NLO χ^2_{pred}	NLO χ^2_{new}	NNLO χ^2_{pred}	NNLO χ^2_{new}
$\sigma_{t\bar{t}}$ Tevatron +CMS+ATLAS	18	19.6	20.5	14.7	15.5
LHCb 7 TeV $W + Z$	33	50.1	45.4	37.1	36.7
LHCb 8 TeV $W + Z$	34	77.0	58.9	76.1	67.2
LHCb 8TeV e	17	37.4	33.4	30.0	27.8
CMS 8 TeV W	22	32.6	18.6	57.6	29.4
CMS 7 TeV $W + c$	10	8.5	10.0	8.7	8.0
D0 e asymmetry	13	22.2	21.5	27.3	22.9
total	3738/3405	4375.9	4336.1	3768.0	3739.3

$$x u_s(x, \mu_0^2) = \bar{u}_s(x, \mu_0^2) = A_{us}(1-x)^{\alpha_{us}} x^{\beta_{us} + \gamma_{us} x^{\delta_{us}}},$$

$$x d_s(x, \mu_0^2) = \bar{d}_s(x, \mu_0^2) = A_{ds}(1-x)^{\beta_{ds}} x^{\alpha_{ds} + \gamma_{ds} x^{\delta_{ds}}},$$

$\bar{d} \neq \bar{u}$ at small x
(the same applies for CT14)

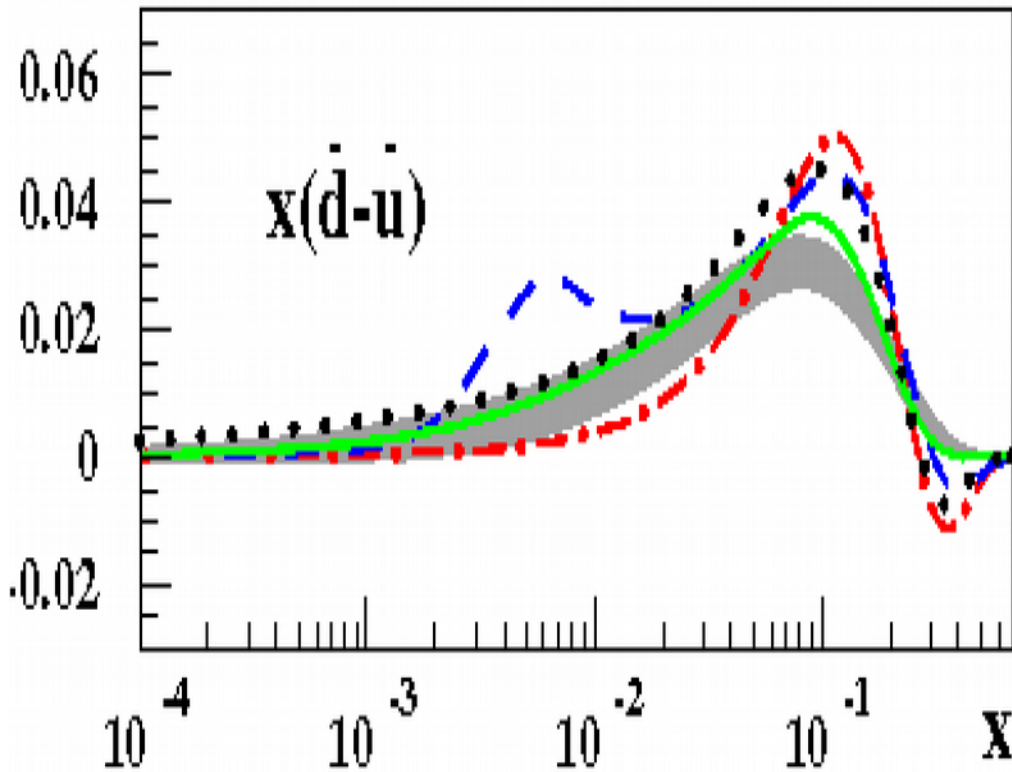
The sum of χ^2/NDP for the DY data by LHCb, CMS, and D0 from the table:

184/119 (MMHT16)

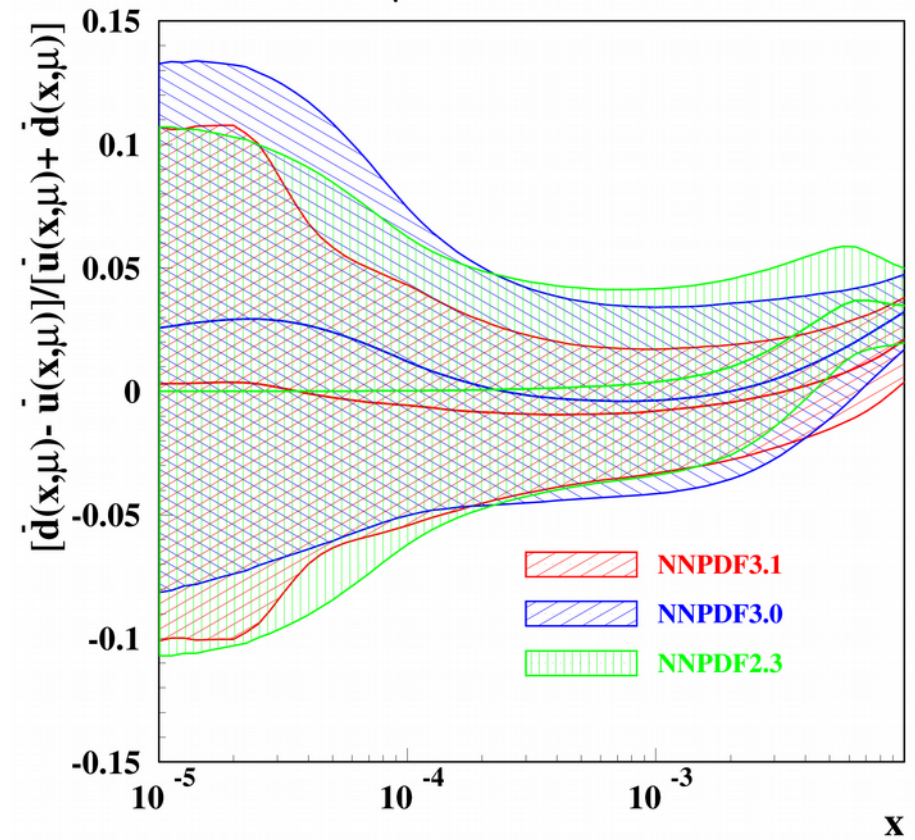
171/119 (ABMP16, no filtering), account of other DY data increases the difference

Sea quark iso-spin asymmetry

$\mu=3 \text{ GeV}$



ABM12 CT10 JR09 MSTW08 NNPDF2.3



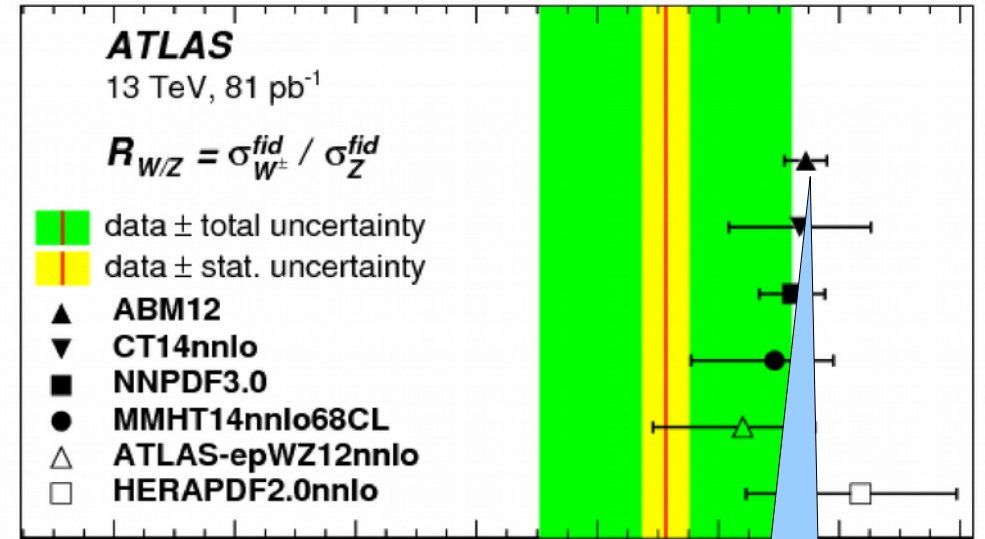
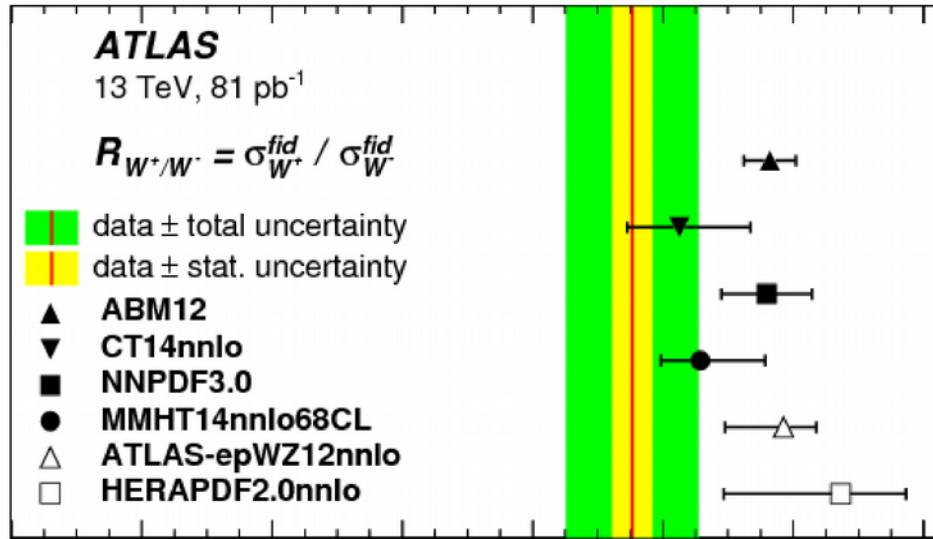
sa, Blümlein, Moch PRD 89, 054028 (2014)

- At $x \sim 0.1$ the sea quark iso-spin asymmetry is controlled by the fixed-target DY data (E-866), weak constraint from the DIS (NMC)
- At $x < 0.01$ Regge-like constraint like $x^{(a-1)}$, with a close to the meson trajectory intercept; the “unbiased” NNPDF fit follows the same trend

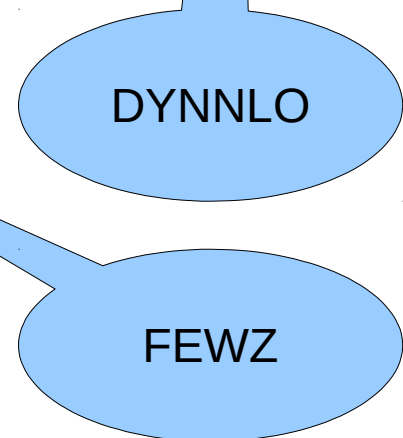
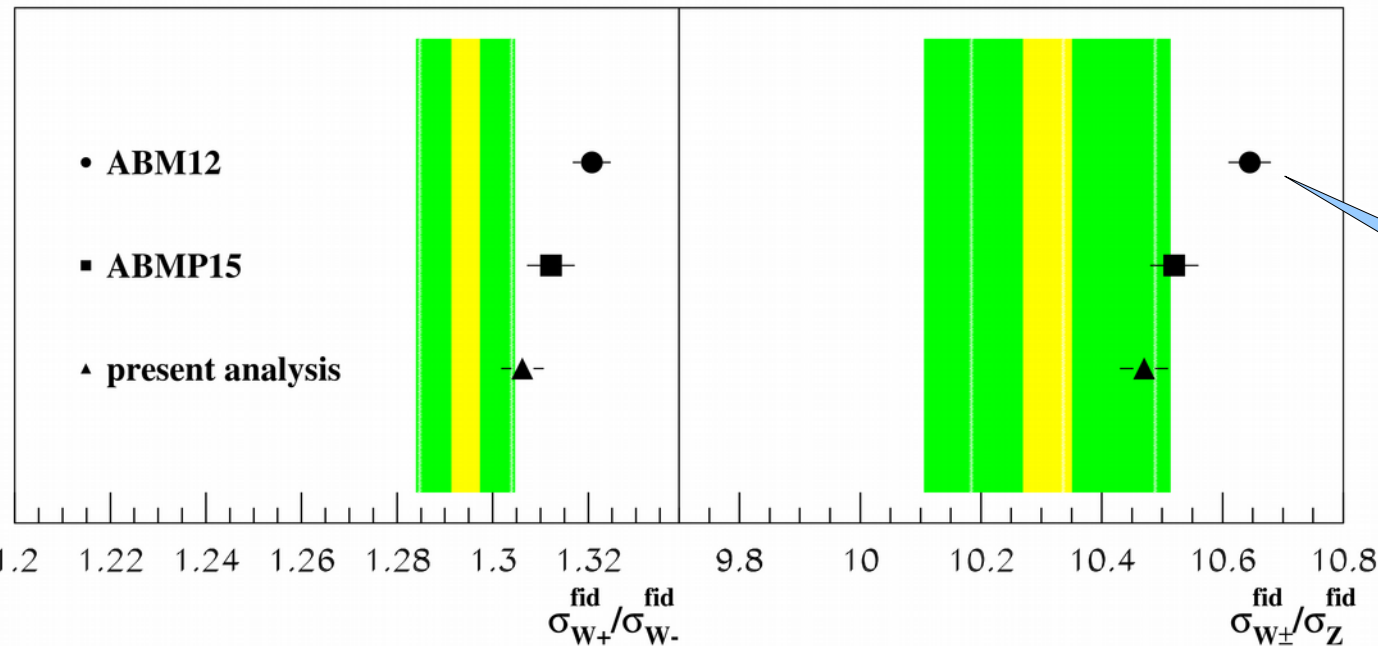
Onset of the Regge asymptotics is out of control

ATLAS W&Z at 13 TeV

ATLAS, hep-ex/1603.09222

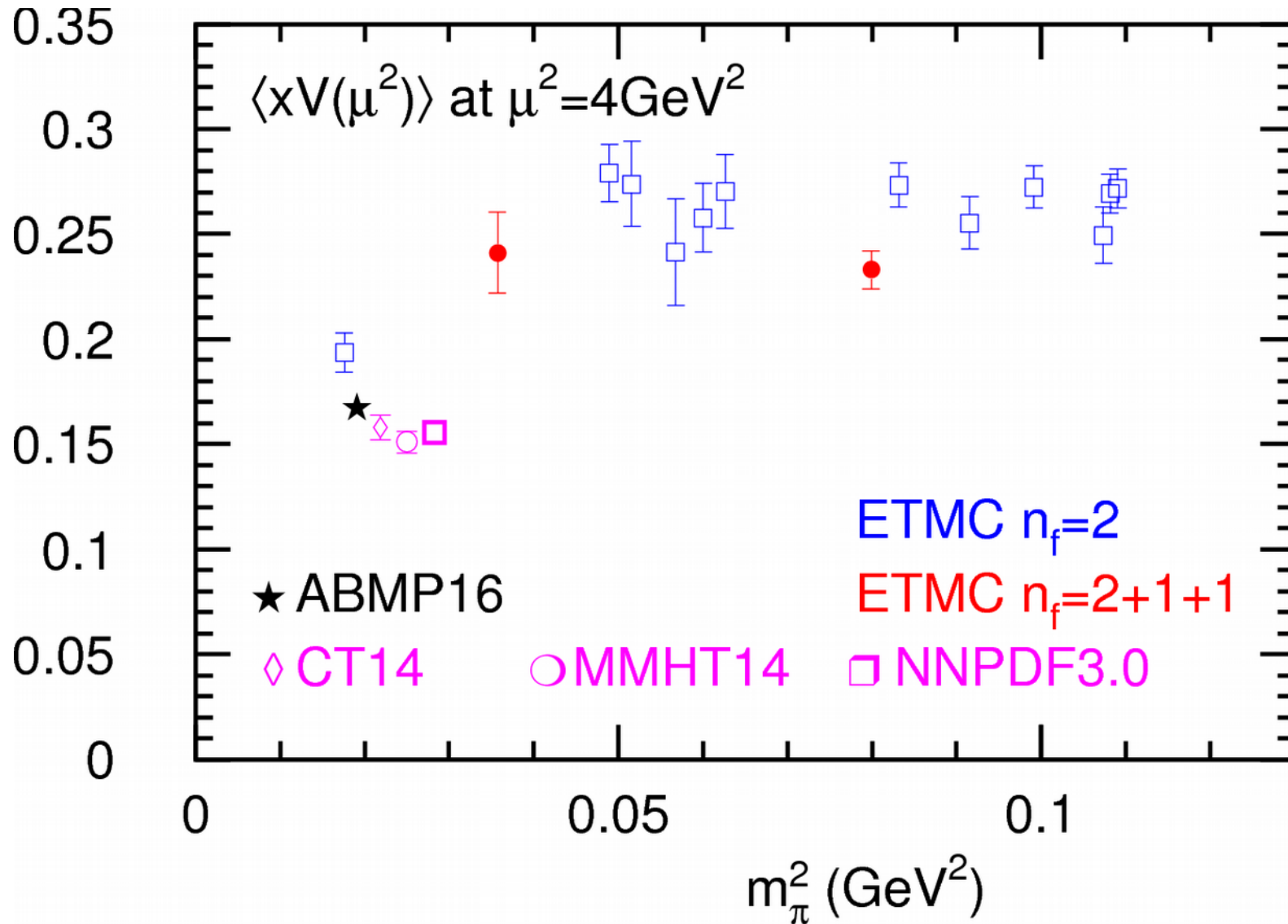


ATLAS (13 TeV, 81 pb⁻¹) 1603.09222



Data are well accommodated into the fit $\chi^2/NDP=9/6$

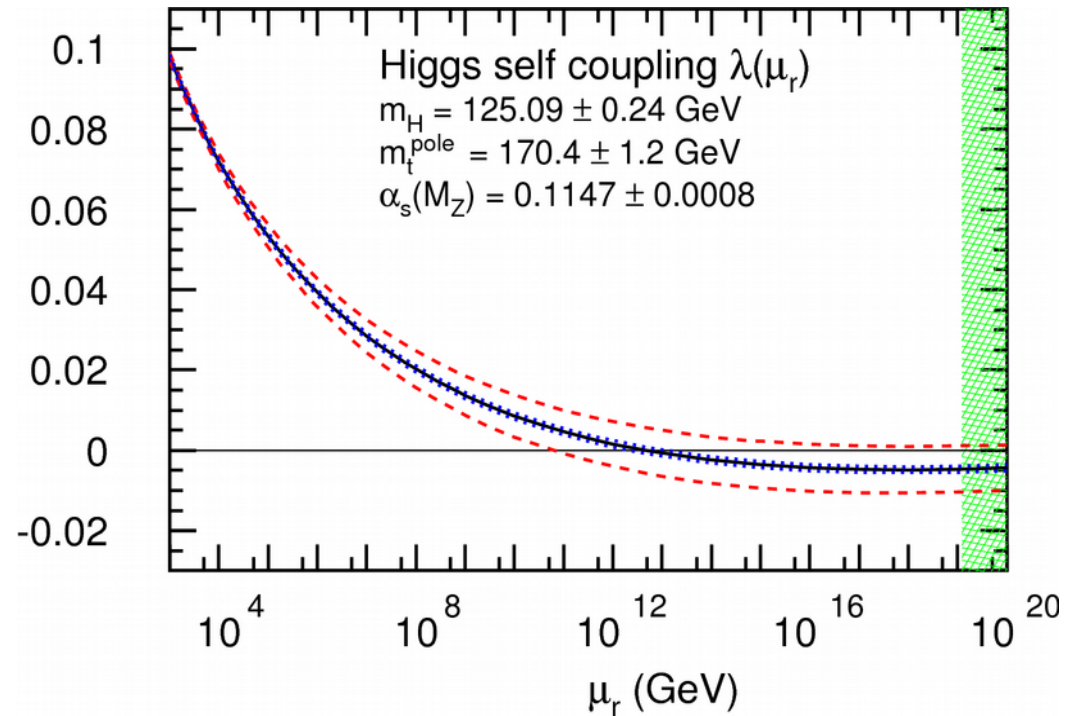
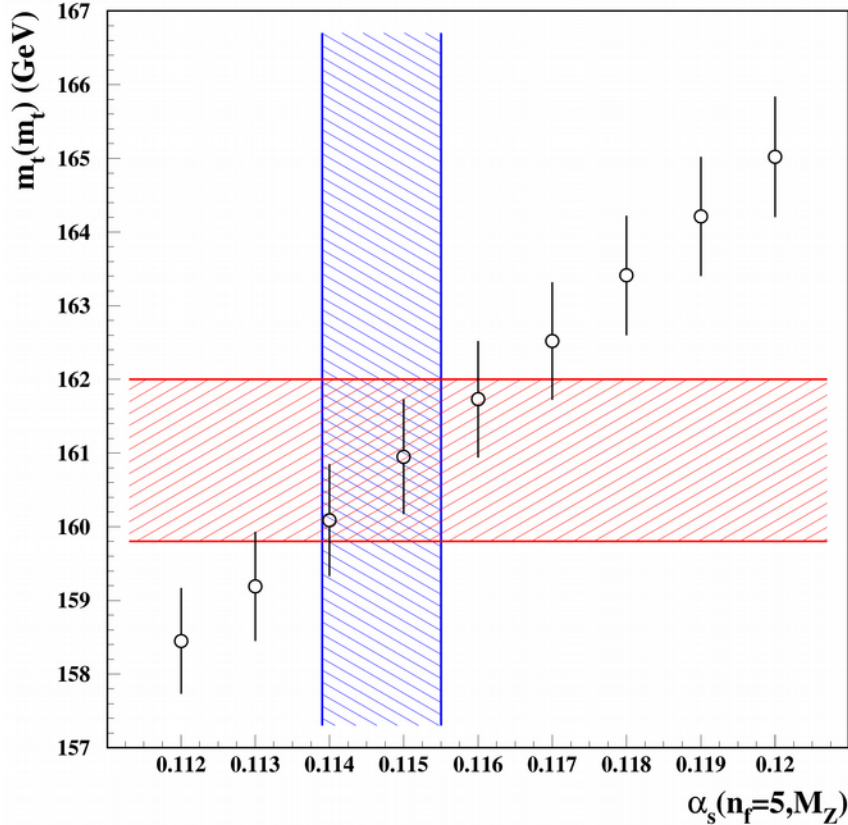
Comparison with lattice results



Electroweak vacuum stability

$$m_H = 129.6 \text{ GeV} + 1.8 \times \left(\frac{m_t^{\text{pole}} - 173.34 \text{ GeV}}{0.9} \right) - 0.5 \times \left(\frac{\alpha_s^{(n_f=5)}(M_Z) - 0.1184}{0.0007} \right) \text{ GeV} \pm 0.3 \text{ GeV},$$

Buttazzo et al., JHEP 12, 089 (2013)



$$m_t(m_t) = 160.9 \pm 1.1 (\text{exp.}) \text{ GeV}$$

$$m_t^{\text{pole}} = 170.4 \pm 1.2 (\text{exp.}) \text{ GeV}$$

$$\alpha_s(M_Z) = 0.1147(8) \quad \text{NNLO}$$

mr: Kniehl, Pikelner, Veretin CPC 206, 84 (2016)

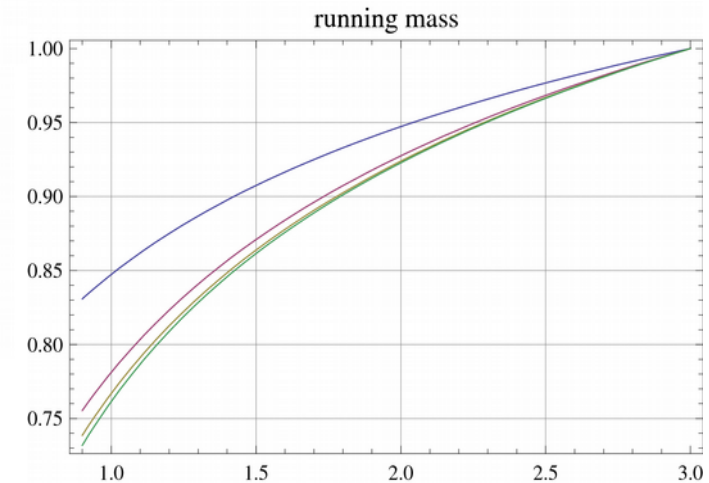
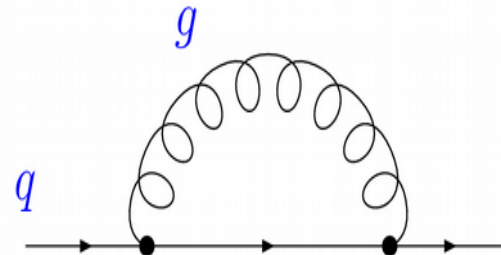
Vacuum stability is quite sensitive to the t -quark mass; stability is provided up to Planck-mass scale

Running mass in DIS

The pole mass is defined for the free (*unobserved*) quarks as a the QCD Lagrangian parameter and is commonly used in the QCD calculations

$$\mathcal{L} = -\frac{1}{4} F_{\mu\nu} F^{\mu\nu} + \sum_{\text{flavors}} \bar{q} (i\not{D} - m_q) q$$

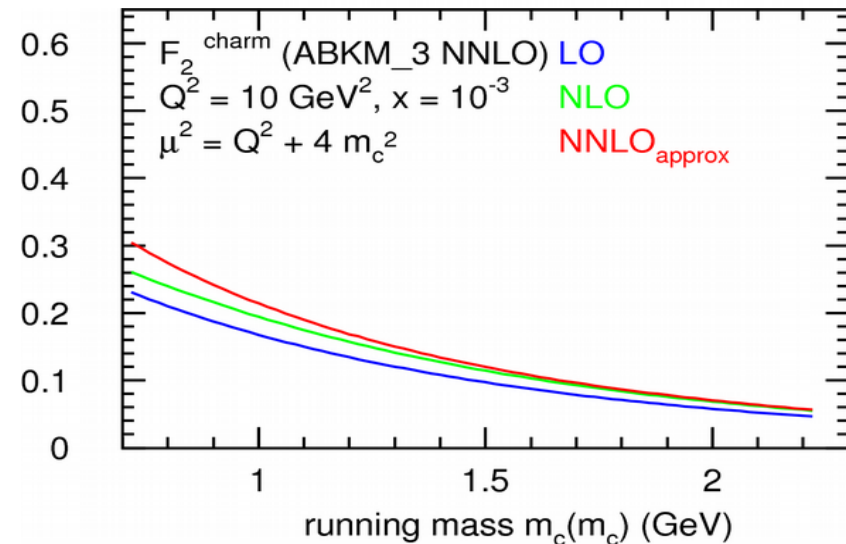
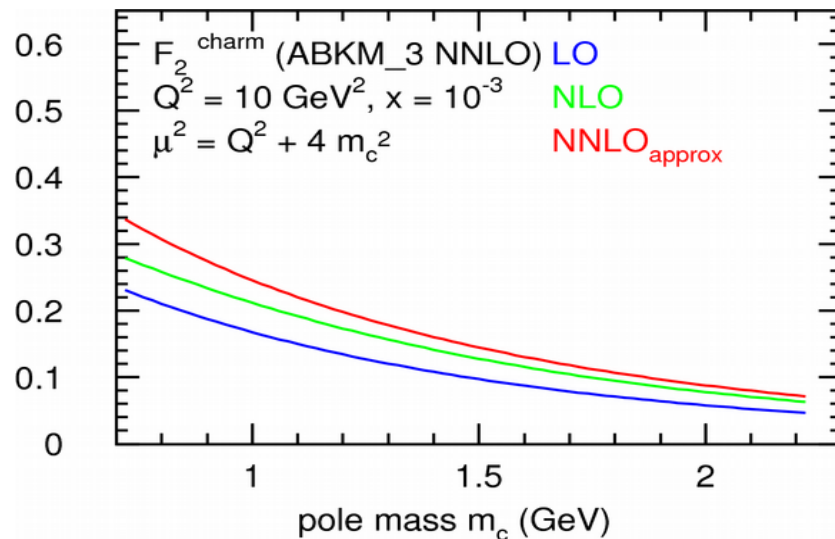
$$\not{p} - m_q - \Sigma(p, m_q) \Big|_{p^2=m_q^2}$$



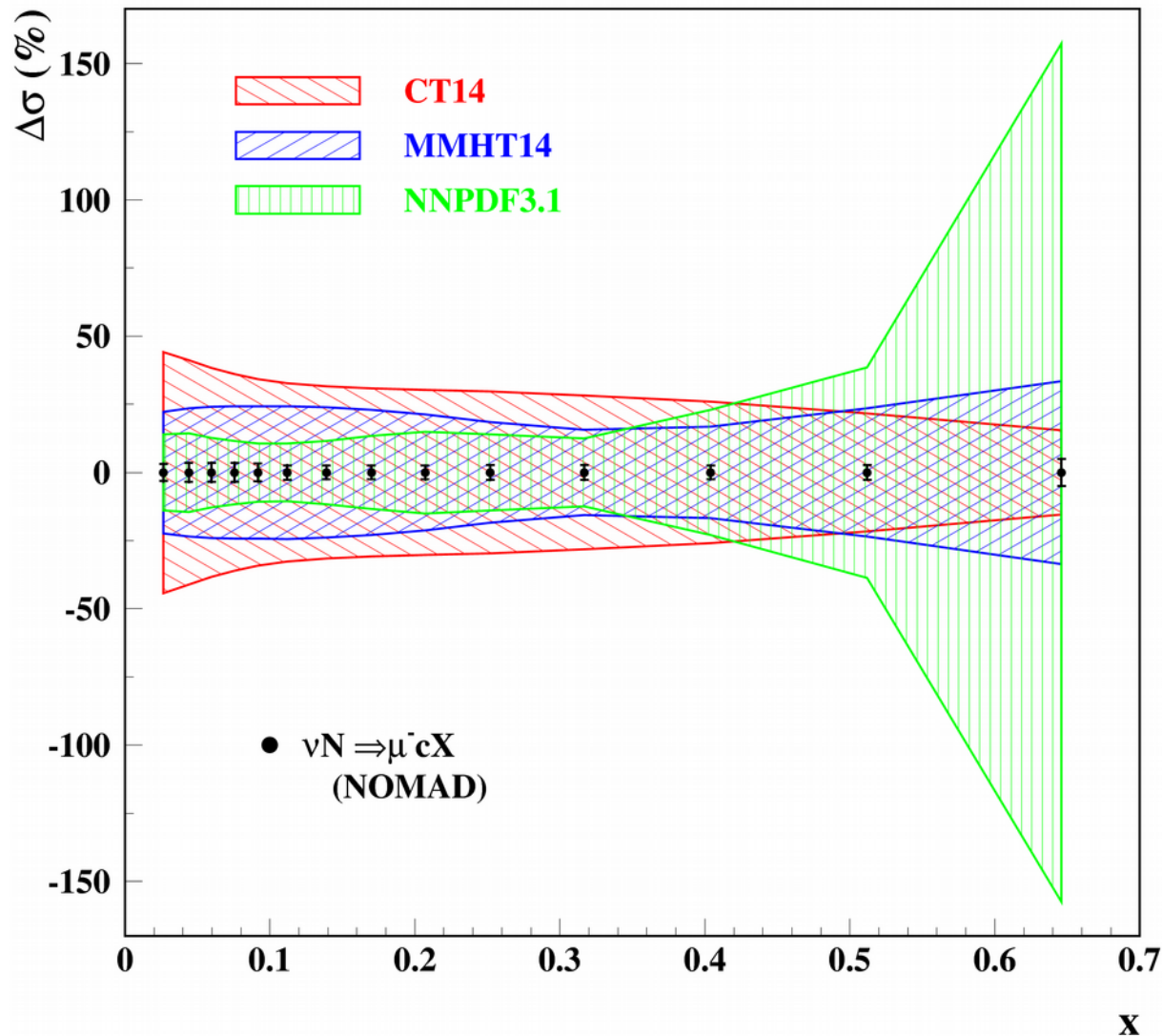
The quantum corrections due to the self-energy loop Integrals receive contribution down to scale of $O(\Lambda_{\text{QCD}})$

→ sensitivity to the high order corrections, particularly at the production threshold

$$\mu^2 \frac{d}{d\mu^2} m(\mu) = \gamma(\alpha_s) m(\mu)$$



Impact of NOMAD data



- Evident room for the PDF improvement by adding NOMAD data to various PDF fits
- Big spread in the predictions \Rightarrow PDF4LHC averaging provides inefficient estimate